Computing the projected reachable set of stochastic biochemical reaction networks modelled by switched affine systems

Francesca Parise, Maria Elena Valcher and John Lygeros

***Abstract*—A fundamental question in systems biology is what combinations of mean and variance of the species present in a stochastic biochemical reaction network are attainable by perturbing the system with an external signal. To address this question, we show that the moments evolution in any generic network can be either approximated or, under suitable assumptions, computed exactly as the solution of a switched affine system. We then propose a new method to approximate the reachable set of such switched affine system. A remarkable feature of our approach is that it allows one to easily compute projections of the reachable set for pairs of moments of interest, without requiring the computation of the full reachable set, which can be prohibitive for large networks. As a second contribution, we also show how to select the external signal in order to maximize the probability of reaching a target set. To illustrate the method we study a renown model of controlled gene expression and we derive estimates of the reachable set, for the protein mean and variance, that are more accurate than those available in the literature and consistent with experimental data.**

I. Introduction

One of the most impressive results achieved by synthetic biology in the last decade is the introduction of externally controllable modules in biochemical reaction networks. These are biochemical circuits that react to external signals, as for example light pulses [1], [2], [3] or concentration signals [4], [5], allowing researchers to influence and possibly control the behavior of cells *in vivo*. To fully exploit these tools, it is important to first understand what range of behaviors they can exhibit under different choices of the external signal. For deterministic systems, this amounts to computing the set of states that can be reached by the controlled system trajectories starting from a known initial configuration [6], [7]. Since chemical species are often present in low copy numbers inside the cell, biochemical reaction networks can however be inherently stochastic [8]. In other words, if we apply the same signal to a population of identical cells, then every cell will have a different evolution (with different likelihood), requiring a probabilistic analysis.

F. Parise is with the Laboratory for Information and Decision Systems, MIT, Cambridge, MA: parisef@mit.edu, M.E. Valcher is with the Department of Information Engineering, University of Padova, Italy: meme@dei.unipd.it and J. Lygeros is with the Automatic Control Laboratory, ETH, Zurich, Switzerland: lygeros@control.ee.ethz.ch. We thank M. Khammash for allowing us to perform the experiments in the CTSB Laboratory, ETH, J. Ruess and A.M. Argeitis for their help in collecting the data of Fig. 6a) and M. Althoff for his assistance with the use of CORA. Research partially supported by the Swiss National Science Foundation (grant P2EZP2_168812).

If we interpret each cell as an independent realization, we can then study the effect of the external signal on a population of cells by characterizing how such a signal influences the moments of the underlying stochastic process. Specifically, in this paper we pose the following question:

"What combinations of moments of the stochastic process can be achieved by applying the external signal?"

This approach is motivated for example by biotechnology applications, where one would like to control the average behavior of the cells in large populations, instead of each cell individually [1], [2], [3], [4], [5], [9], [10], [11]. More on the theoretical side, this perspective can be useful to investigate fundamental questions on the role of noise in stochastic biochemical reaction networks, as in the seminal work [12]. It is well known for example that gene expression noise can be beneficial for some cell functions and damaging for others. For instance, [13] found that cell-to-cell variability due to gene expression noise can lead to significant improvements in the response of a population to antibiotic challenges. On the other hand, some processes, as the ones related to organisms development, rely on precise spatial and temporal events sequencing and are thus very sensitive to noise [14]. To this day, researchers are not unanimous on whether in natural circuits the amount of gene expression noise is subject to universal scaling laws (the most common conjecture being that $CV^2 = 1/\mathbb{E}[\text{mRNA}]$) or whether it is dependent on the promoter architecture (and thus subject to natural selection) [15]. Being able to exploit externally controllable modules as the ones considered in this paper to artificially tune the level of noise in a system, can be fundamental to help researchers understand the causes and most importantly the consequences of gene expression noise. The method suggested in this paper is a first step in this direction since it allows one to quantify the levels of noise (e.g. the mean and variance combinations) achievable by externally controllable modules, thus enabling their use in future research.

The cornerstone of our approach is the observation that while the number of copies in each cell is stochastic, the evolution of the moments is deterministic. Consequently, the above question can be reformulated as a reachability problem in the moment space. To address such a problem we exploit two specific properties of the application at hand:

P1) *Projected reachable set:* biologists are often interested in analyzing the behavior of only a few chemical species of the possibly many involved in the network. Consequently,

one is usually only interested in computing the projection of the reachable set (which is a high-dimensional object) on some low-dimensional space of interest.

P2) *Input structure:* we consider controlled biochemical networks which are used in finite-time experiments. Consequently, we are interested in the finite-time reachable set and we assume that the external signal can change only at K pre-assigned instant of times, for example corresponding to measurements or cell dilutions, within a finite set of cardinality I.

Thanks to P2), the moments evolution can be either described or approximated by a switched affine system (with I modes and K fixed switching instants). Our first contribution is to propose a method to approximate the reachable set of such a switched affine system by exploiting its specific structure, that is, the fact that the switching signal is a control variable and that the dynamics in each mode are autonomous and affine. Our method is an extension of the hyperplane method, originally proposed in [16] for linear system, and allows one to compute directly the projection of the reachable set, without requiring the computation of the entire reachable set first, thus fully exploiting P1). Our core contribution is to outsource the complexity of computing the constants required by the hyperplane method, which depend on the exponential number of possible sequences, to a mixed integer linear program (MILP) solver. More precisely, switching between I modes at K time-points leads to I^K different switching inputs. Our MILP formulation involves only $(I+1)K$ continuous variables and IK discrete variables. The heavy lifting is thus done by the MILP solver, for which powerful standard tools are readily available [17], [18]. A detailed comparison of our method with the vast literature on reachability analysis is given in Section III-C.

As a second contribution we show how to apply the proposed reachability method to biochemical reaction networks by distinguishing two cases:

1) If all the reactions follow the laws of mass action kinetics and are at most of order one, the system of moments equations is switched affine. Consequently, for this class of networks, the above question can be solved by directly applying the newly suggested hyperplane method in the moments space;
2) For all other reaction networks the moments equations are in general non-closed (i.e., the evolution of mean and variance depends on higher order moments). We show however that the evolution of the probability of being in a given state can be described by an *infinite* dimensional switched system and that the desired moments can be computed as the output of such system. We then show: i) How to approximate such an infinite dimensional system with a finite dimensional one, by extending the finite state projection method [19] to controllable networks, ii) How to compute the reachable set of the finite dimensional system by applying the newly suggested hyperplane method in the probability space, and iii) How to recover an approximation of the original reachable set from the reachable set of the finite dimensional system.

As a third contribution, in the last part of the paper we change perspective and, instead of focusing on population properties, we consider the behaviour of a single cell (i.e., a single realization of the process), given a fixed initial condition or an initial probability distribution. Such perspective has been commonly employed for the case without external signals, see e.g. [19], [20], [21], [22]. Our objective is to show how the external signal can be used to control single cell realizations by posing the following question

"What external signal should be applied to maximize the probability that the cell trajectory reaches a prespecified subset of the state space at the end of the experiment?"

We show that such a problem can be addressed by using similar tools as those derived for the population analysis.

Outline: In Section II we present the hyperplane method. In Section III-A we review how to compute the hyperplane constants for linear systems, while in Section III-B we propose a new procedure for switched affine systems. We compare our method with the literature in Section III-C and comment on possible extensions to infinite reachable sets in Section III-D. In Section IV we introduce stochastic biochemical reaction networks and the controlled chemical master equation (CME). Additionally, we recap how to derive the moments equations from the CME (Section IV-A) and we derive an extension of the finite state projection method to controlled biochemical networks (Section IV-B). In Section V we show how to compute the reachable set of biochemical networks and in Section VI we derive the results on single cell realizations. Section VII illustrates our theoretical results on a gene expression case study.

We note that part of the results of this paper appeared in our previous works [23], [24]. Specifically, in [23] we first suggest the use of the hyperplane method to compute the reachable set of biochemical networks with *linear* moment equations, which we then adapted in [24] to the case of *switched affine* moment equations. As better detailed in Section IV-A, the assumptions made both in [23] and [24] do not allow for bimolecular reactions, which are instead present in the vast majority of biochemical networks. The key contribution of this paper is the generalisation of our analysis to *any* biochemical network by using the approach described in point 2) above. The analysis of single cell realizations is also entirely new.

Notation: Given $a < b \in \mathbb{N}$, we set $\mathbb{N}[a,b] := \{a, a+1, \dots, b\}$. Given a set $\mathcal{S}$, the symbol $\partial\mathcal{S}$ denotes its boundary, $\text{conv}(\mathcal{S})$ its convex hull and $|\mathcal{S}|$ its cardinality. For a vector $x \in \mathbb{R}^n$, $x_p := [x]_p$ denotes its pth component, $|x| := [|x_1|^\top, \dots, |x_n|^\top]^\top$ and $\|x\|_\infty := \max_{p=1,2,\dots,n} |x_p|$ denotes the infinity norm. $\mathbb{1}$ denotes a vector of all ones, e_i is the ith canonical vector. Given two random variables Z_1, Z_2, we denote by $\mathbb{V}[Z_1]$ and $\mathbb{V}[Z_1, Z_2]$ their variance and covariance.

II. Reachability tools

A. The reachable set and the hyperplane method

Consider the n-dimensional nonlinear control system

$$\dot{x}(t) = f(x(t), \sigma(t)), \quad t \geq 0, \tag{1}$$

where x is the n-dimensional state and σ the m-dimensional input function. Set a final time $T > 0$ and let $\mathcal{S}$ be *the set of admissible input functions* that map $[0, T]$ into $\mathbb{R}^m$. We assume that the function $f : \mathbb{R}^n \times \mathbb{R}^m \to \mathbb{R}^n$ is such that, for every initial condition $x(0) \in \mathbb{R}^n$ and every input function $\sigma \in \mathcal{S}$, the solution of (1), denoted by $x(t; x(0), \sigma), t \geq 0$, is well defined and unique at every time $t \geq 0$. The reachable set of system (1) at time T is defined as the set of all states $x \in \mathbb{R}^n$ that can be reached at time T, starting from $x(0)$, by using an admissible input function $\sigma \in \mathcal{S}$.

Definition 1 (Reachable set at time T)**.** *The reachable set at time $T > 0$ from $x(0) = x_0$, for system* (1) *with admissible input set $\mathcal{S}$, is*

$$\mathcal{R}_T(x_0) := \{x \in \mathbb{R}^n \mid \exists\ \sigma \in \mathcal{S} : x = x(T; x_0, \sigma)\}. \quad (2)$$

One can show that under mild assumptions (see e.g. Filippov's theorem, [25, pg 119]) the set $\mathcal{R}_T(x_0)$ is compact. We show in the subsequent Corollaries 1 and 2 that this is indeed the case for the linear and switched affine systems considered in this paper. Computing the reachable set for nonlinear systems is in general a very difficult task. For the case of linear systems with bounded inputs a method to construct an outer approximation of $\mathcal{R}_T(x_0)$ as the intersection of a family of half-spaces that are tangent to its boundary (see Fig. 1) was proposed in [16].

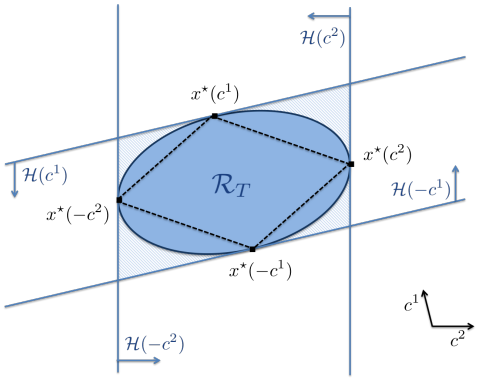

Fig. 1. Illustration of the hyperplane method for a *convex* reachable set $\mathcal{R}_T(x_0)$ (in blue). The external parallelogram is the outer approximation, the region in between the dotted lines is the inner approximation.

We present here a generalisation of this method to system (1). For a given direction $c \in \mathbb{R}^n$, let us define

$$v_T(c) := \max_{x \in \mathcal{R}_T(x_0)} c^\top x, \quad (3)$$

where, for simplicity, we omitted the dependence of $v_T(c)$ on the initial condition x_0. Let

$$\mathrm{H}_T(c) := \{x \in \mathbb{R}^n \mid c^\top x = v_T(c)\} \quad (4)$$

be the corresponding hyperplane. By definition of the constant $v_T(c)$, the associated half-space

$$\mathcal{H}_T(c) := \{x \in \mathbb{R}^n \mid c^\top x \leq v_T(c)\} \quad (5)$$

is a superset of $\mathcal{R}_T(x_0)$. We note that if $\partial\mathcal{R}_T(x_0)$ is smooth, then $\mathrm{H}_T(c)$ is the tangent plane to $\partial\mathcal{R}_T(x_0)$. By evaluating the above hyperplanes and half-spaces for various directions, one can construct an outer approximation of the reachable set, as illustrated in the next theorem. If the reachable set is convex then an inner approximation can also be derived.

Theorem 1 (The hyperplane method [16])**.** *Given system* (1)*, an initial condition $x_0 \in \mathbb{R}^n$, a fixed time $T > 0$, an integer number $D \geq 2$, and a set of D directions $\mathcal{C} := \{c^1, \ldots, c^D\}$, define the half-spaces $\mathcal{H}_T(c^d)$ as in* (5)*, for $d = 1, \ldots, D$.*

1) The set

$$\mathcal{R}_T^{out}(x_0) := \cap_{d=1}^{D} \mathcal{H}_T(c^d)$$

is an outer approximation of the reachable set $\mathcal{R}_T(x_0)$ at time T starting from x_0.

2) If the set $\mathcal{R}_T(x_0)$ is convex and for each $d = 1, 2, \ldots, D$, we select a (tangent) point

$$x_T^\star(c^d) \in \mathcal{R}_T(x_0) \cap \mathrm{H}_T(c^d) \quad (6)$$

then the set

$$\mathcal{R}_T^{in}(x_0) := \mathrm{conv}\left(\{x_T^\star(c^d), d = 1, 2, \ldots, D\}\right)$$

is an inner approximation of the reachable set $\mathcal{R}_T(x_0)$ at time T starting from x_0. □

Remark 1. *We note that by construction the outer approximation $\mathcal{R}_T^{out}(x_0)$ is a convex object. Specifically, when the number of hyperplanes tends to infinity and their normal vectors sample uniformly the ball of any norm then $\mathcal{R}_T^{out}(x_0)$ approximates exactly the* convex hull *of $\mathcal{R}_T(x_0)$ (which is an outer approximation of $\mathcal{R}_T^{out}(x_0)$ itself). Similarly, for* any *set $\mathcal{R}_T(x_0)$, the set $\mathcal{R}_T^{in}(x_0)$ is an inner approximation of the convex hull of $\mathcal{R}_T(x_0)$. However, the inner approximation of the convex hull of a set is an inner approximation of the set itself only if such set is convex, as assumed in the previous theorem.* □

The main advantage of this method is that hyperplanes are very easy objects to handle and visualise. The main disadvantage is that the higher the dimension n of the state space, the higher in general is the number of directions D required to obtain a good characterisation of the reachable set. In the next subsection we show that, in cases when only the projection of the reachable set on a plane is needed, one can consider only hyperplanes that are perpendicular to the plane of interest, thus reducing significantly the computational effort.

B. The output reachable set

Let the output of system (1) be

$$y(t) = Lx(t), \quad (7)$$

for $L \in \mathbb{R}^{p \times n}$, and the output reachable set be the set of all output values that can be generated at time T from $x(0) = x_0$, by using an admissible input function $\sigma \in \mathcal{S}$.

Definition 2 (Output reachable set at time T)**.** *The output reachable set $\mathcal{R}_T^y(x_0)$* from x_0 at time $T > 0$*, for system* (1) *with admissible input set $\mathcal{S}$ and output as in* (7)*, is*

$$\mathcal{R}_T^y(x_0) := \{y \in \mathbb{R}^p \mid \exists\ x \in \mathcal{R}_T(x_0) : y = Lx\}.$$

For simplicity, in the following we restrict our discussion to the case of a two-dimentional output vector, that is

$$y(t) = Lx(t) = \begin{bmatrix} l_1^\top x(t) \\ l_2^\top x(t) \end{bmatrix} \in \mathbb{R}^2, \tag{8}$$

for some $l_1, l_2 \in \mathbb{R}^n$, the generalization to higher dimentions is however immediate. Note that, for any pair of indices $i, j \in \{1, \dots, n\}, i \neq j$, one can recover the projection of the reachable set $\mathcal{R}_T(x_0)$ onto an (x_i, x_j)-plane of interest by imposing $l_1 = e_i$ and $l_2 = e_j$. The two-dimentional output vector case can therefore be applied to study the relation between the mean behavior of two species or between mean and variance of a single species in large biochemical networks.

In the following theorem we show that inner and outer approximations of $\mathcal{R}_T^y(x_0)$ can be computed by selecting only hyperplanes that are perpendicular to the plane of interest.

Theorem 2 (Projection on a two dimensional subspace)**.** *Consider system* (1)*, with output* (8) *and initial condition* $x_0 \in \mathbb{R}^n$*. Let* $T > 0$ *be a fixed time,* $D \geq 2$ *an integer number and choose* D *values* $\gamma^d \in \mathbb{R}$*. Set* $c^d := l_2 - \gamma^d l_1 \in \mathbb{R}^n$ *and*

$$\mathcal{H}_T^{y,up}(\gamma^d) := \{y \in \mathbb{R}^2 \mid y_2 \leq \gamma^d y_1 + v_T(c^d)\},$$
$$\mathcal{H}_T^{y,low}(\gamma^d) := \{y \in \mathbb{R}^2 \mid y_2 \geq \gamma^d y_1 - v_T(-c^d)\},$$

where $v_T(c^d)$ *are as in* (3)*. Then the set*

$$\mathcal{R}_T^{y,out}(x_0) := \cap_{d=1}^D [\mathcal{H}_T^{y,up}(\gamma^d) \cap \mathcal{H}_T^{y,low}(\gamma^d)] \tag{9}$$

is an outer approximation of $\mathcal{R}_T^y(x_0)$*. Moreover, if* $\mathcal{R}_T(x_0)$ *is convex then the set*

$$\mathcal{R}_T^{y,in}(x_0) := \text{conv}\left(\{Lx_T^\star(c^d), Lx_T^\star(-c^d), d = 1, 2, \dots, D\}\right), \tag{10}$$

where $x_T^\star(c^d)$ *is defined as in* (6)*, is an inner approximation of* $\mathcal{R}_T^y(x_0)$*.* □

Proof: By definition, for any $\bar{y} \in \mathcal{R}_T^y(x_0)$ there exists an $\bar{x} \in \mathcal{R}_T(x_0)$ such that $\bar{y}^\top = [l_1^\top \bar{x}, l_2^\top \bar{x}]$. By Theorem 1, for any direction c^d it holds that $\mathcal{R}_T(x_0) \subset \mathcal{H}_T(c^d)$. Consequently, $\bar{x} \in \mathcal{R}_T(x_0)$ implies $\bar{x} \in \mathcal{H}_T(c^d)$. By substituting the definition of c^d given in the statement we get

$$\bar{x} \in \mathcal{H}_T(c^d) \Leftrightarrow (c^d)^\top \bar{x} \leq v_T(c^d) \Leftrightarrow$$
$$\Leftrightarrow (l_2 - \gamma^d l_1)^\top \bar{x} \leq v_T(c^d) \Leftrightarrow l_2^\top \bar{x} \leq \gamma^d l_1^\top \bar{x} + v_T(c^d).$$

The last inequality implies that $\bar{y}^\top = [l_1^\top \bar{x}, l_2^\top \bar{x}]$ satisfies $\bar{y}_2 \leq \gamma^d \bar{y}_1 + v_T(c^d)$. Hence $\bar{y} \in \mathcal{H}_T^{y,up}(\gamma^d)$. By applying the same reasoning for the direction $-c^d$ one gets $-\bar{y}_2 \leq -\gamma^d \bar{y}_1 + v_T(-c^d)$ or equivalently $\bar{y}_2 \geq \gamma^d \bar{y}_1 - v_T(-c^d)$. Hence $\bar{y} \in \mathcal{H}_T^{y,low}(\gamma^d)$. Consequently, $\mathcal{R}_T^y(x_0) \subseteq \mathcal{H}_T^{y,up}(\gamma^d) \cap \mathcal{H}_T^{y,low}(\gamma^d)$ for any γ^d and therefore $\mathcal{R}_T^y(x_0) \subseteq \mathcal{R}_T^{y,out}(x_0)$. If $\mathcal{R}_T(x_0)$ is convex, then $\mathcal{R}_T^y(x_0)$ is convex as well. The points $Lx_T^\star(c^d)$ and $Lx_T^\star(-c^d)$ belong to $\mathcal{R}_T^y(x_0)$ by construction. Consequently, by convexity, it must hold that $\mathcal{R}_T^{y,in}(x_0) \subseteq \mathcal{R}_T^y(x_0)$. ■

III. Computing the tangent hyperplanes

The success of the hyperplane method hinges on the possibility of efficiently evaluating, for any given direction c, the constant $v_T(c)$ in (3). Note that this problem is equivalent to the following finite time optimal control problem

$$\begin{aligned} v_T(c) := \max_{\sigma \in \mathcal{S}} \quad & c^\top x(T) \\ \text{s.t.} \quad & \dot{x}(t) = f(x(t), \sigma(t)), \quad \forall t \in [0, T], \\ & x(0) = x_0. \end{aligned} \tag{11}$$

In the rest of this section, we aim at solving (11) for systems with the specific structure needed to analyse biochemical reaction networks. To this end, we start by extending in Section III-A the result originally derived in [16] for linear systems with continuous inputs to linear systems with discrete inputs. This extension is needed because in most biological applications the input is indeed discrete (see e.g. the gene expression system discussed in Section VII-A1, where the input is of the ON/OFF type). Linear systems can only be used to describe the moment evolution of a restricted class of biochemical networks. In the subsequent Section IV we show that in general one obtains a switched affine system. In Section III-B we suggest a method to solve (11) for such a class of switched affine systems.

A. Linear systems with bounded input

The hyperplane method was originally proposed for linear systems with bounded inputs

$$\dot{x}(t) = Ax(t) + B\sigma(t), \tag{12}$$

where $x(t) \in \mathbb{R}^n$, $A \in \mathbb{R}^{n \times n}$, $B \in \mathbb{R}^{n \times m}$ and $\sigma(t) \in \mathbb{R}^m$. Since biological signals are non-negative and bounded, we here make the following assumption on the input set $\mathcal{S}$.

Assumption 1. *The input function* σ *belongs to the admissible set* $\mathcal{S}_\Sigma := \{\sigma \mid \sigma(t) \in \Sigma, \forall t \in [0, T]\}$*, where* $\Sigma = \Sigma_1 \times \ldots \times \Sigma_m$*. Moreover, there exist* $\bar{\sigma}_r > 0, r \in \mathbb{N}[1, m]$*, such that either (a) every set* Σ_r *is the interval* $\Sigma_r^c := [0, \bar{\sigma}_r]$ *(continuous and bounded input set), or (b) for every set* Σ_r *there exists* $2 \leq q_r < +\infty$ *such that* $\Sigma_r^d := \left\{\sigma_r^1, \sigma_r^2, \dots, \sigma_r^{q_r}\right\} \subset \mathbb{R}_{\geq 0}$ *(finite input set), with the convention* $\sigma_r^1 < \sigma_r^2 < \ldots < \sigma_r^{q_r}$*,* $\sigma_r^1 = 0$ *and* $\sigma_r^{q_r} = \bar{\sigma}_r$*. We set* $\Sigma^c := \Sigma_1^c \times \ldots \times \Sigma_m^c$*,* $\Sigma^d := \Sigma_1^d \times \ldots \times \Sigma_m^d$*, and denote by* $\mathcal{S}_{\Sigma^c}$ *and* $\mathcal{S}_{\Sigma^d}$ *the corresponding admissible sets.*

In the case of a continuous and bounded input set, i.e. under Assumption 1-(a), it was shown in [16] that it is possible to solve the control problem in (11) in closed form by using the Maximum Principle [25].

Proposition 1 (Tangent hyperplanes for linear systems with bounded and continuous inputs [16])**.** *Consider system* (12) *and suppose that Assumption 1-(a) holds. Define the following admissible input function, expressed component-wise for every* r*th entry,* $r = 1, \dots, m$*, as*

$$\sigma_r^\star(t) := \begin{cases} \bar{\sigma}_r & \text{if} \quad c^\top e^{A(T-t)} b_r > 0; \\ 0 & \text{if} \quad c^\top e^{A(T-t)} b_r < 0; \\ 0 \leq \sigma_r \leq \bar{\sigma}_r & \text{if} \quad c^\top e^{A(T-t)} b_r = 0; \end{cases} \tag{13}$$

where b_r denotes the rth column of B. Then

$$v_T(c) = c^\top e^{AT} x_0 + \sum_{r=1}^m \bar{\sigma}_r \int_0^T \left[c^\top e^{A(T-t)} b_r\right]_+ dt, \quad (14)$$

where $[g(t)]_+$ denotes the positive part of the function $g(t)$, namely $[g(t)]_+ = g(t)$ when $g(t) > 0$ and zero otherwise. Suppose additionally that the pair (A, b_r) is reachable, for every $r \in \mathbb{N}[1,m]$. Then there exists no interval $[\tau_1, \tau_2]$, with $0 \leq \tau_1 < \tau_2 \leq T$, such that $c^\top e^{A(T-t)} b_r = 0$ for every $t \in [\tau_1, \tau_2]$. Consequently, a tangent point can be obtained as

$$x_T^\star(c) := e^{AT} x_0 + \int_0^T e^{A(T-t)} B \sigma^\star(t) dt. \quad (15)$$

□

By using the explicit characterisation given in Proposition 1 together with Theorems 1 and 2, one can efficiently construct both an inner and an outer approximation of the (output) reachable set for linear systems with *continuous and bounded input set* Σ^c, as summarised in the next corollary. Therein we also prove that the result in [16] can be extended from *continuous and bounded input sets* to *finite input sets* Σ^d.

Corollary 1 (The hyperplane method for linear systems)**.** *Consider system* (12) *and suppose that either Assumption 1-(a) or Assumption 1-(b) holds. Let $v_T(c^d)$ and $x_T^\star(c^d)$ be computed as in* (14) *and* (15)*. Then $\mathcal{R}_T(x_0)$ is compact. Moreover $\mathcal{R}_T^{out}(x_0)$ and $\mathcal{R}_T^{in}(x_0)$ ($\mathcal{R}_T^{y,out}(x_0)$ and $\mathcal{R}_T^{y,in}(x_0)$, resp.) as defined in Theorem 1 (Theorem 2, resp.) are outer and inner approximations of $\mathcal{R}_T(x_0)$ (of $\mathcal{R}_T^y(x_0)$, resp.).*

Proof: In the case of continuous and bounded input, that is, under Assumption 1-(a), it is well known that the (finite-time) reachable set $\mathcal{R}_T(x_0)$ is compact and convex. The statement is therefore a trivial consequence of Theorems 1, 2 and Proposition 1. We here show that the same result holds also under Assumption 1-(b). The proof of this second part follows from the fact that the reachable set $\mathcal{R}_T^c(x_0)$, obtained by using the continuous input set Σ^c, and the reachable set $\mathcal{R}_T^d(x_0)$, obtained by using the discrete input set Σ^d, coincide. To prove this, let $\mathcal{R}_T^{bb}(x_0)$ be the reachable set obtained using $\Sigma_r^{bb} := \{0, \bar{\sigma}_r\}$ for any r, that is, the set of vertices of Σ^c. Consider now an arbitrary point $\bar{x} \in \mathcal{R}_T^c(x_0)$, which is a compact set. By definition there exists an admissible input function in Σ^c that steers x_0 to $\bar{x}$ in time T. Since Σ^c is a convex polyhedron, by [26, Theorem 8.1.2], system (12) with input set Σ^c has the bang-bang with bound on the number of switchings (BBNS) property. That is, for each $\bar{x} \in \mathcal{R}_T^c(x_0)$ there exists a bang-bang input function in Σ^{bb} that reaches $\bar{x}$ in the same time T with a finite number of discontinuities. Thus $\bar{x} \in \mathcal{R}_T^{bb}(x_0)$. Since this is true for any $\bar{x} \in \mathcal{R}_T^c(x_0)$, we get $\mathcal{R}_T^c(x_0) \subseteq \mathcal{R}_T^{bb}(x_0)$. From $\Sigma^{bb} \subseteq \Sigma^d \subseteq \Sigma^c$ we get $\mathcal{R}_T^{bb}(x_0) \subseteq \mathcal{R}_T^d(x_0) \subseteq \mathcal{R}_T^c(x_0)$, concluding the proof. ■

B. Switched affine systems

In this section, we propose an extension of the hyperplane method to the case of a switched affine system of the form

$$\dot{x}(t) = A_{\sigma(t)} x(t) + b_{\sigma(t)}, \quad (16)$$

where the switching signal $\sigma(t) \in \mathbb{N}[1,I]$ is the input function, $I \geq 2$ is the number of modes, $x(t) \in \mathbb{R}^n$ and $A_i \in \mathbb{R}^{n\times n}, b_i \in \mathbb{R}^n$ for all $i \in \mathbb{N}[1,I]$. We make the following assumption.

Assumption 2. *The switching signal $\sigma(t)$ switches K times within the finite set $\mathbb{N}[1,I]$ at fixed switching instants $0 = t_0 < \ldots < t_{K+1} = T$, that is, $\sigma \in \mathcal{S}_I^K$, where*

$$\mathcal{S}_I^K := \{\sigma \mid \sigma(t) = i_k \in \mathbb{N}[1,I], \forall t \in [t_k, t_{k+1}), k \in \mathbb{N}[0,K]\}.$$

For every $k \in \mathbb{N}[0,K]$ and $i \in \mathbb{N}[1,I]$ we define $\bar{A}_i^k := e^{A_i(t_{k+1}-t_k)}$ and $\bar{b}_i^k = [\int_0^{(t_{k+1}-t_k)} e^{A_i\tau} d\tau] b_i$. Moreover, we set $x_k := x(t_k)$. Note that under Assumption 2 the reachable set of system (16) consists of a finite number of points that can be computed by solving the state equations for each possible switching signal. Since the cardinality of the set $\mathcal{S}_I^K$ grows exponentially with K, this approach is however computationally infeasible even for small systems. We here show that, on the other hand, the hyperplane constants defined in (11) can be computed by solving a mixed integer linear program (MILP), thus allowing us to exploit the sophisticated software that has been developed to solve large MILPs in the last years [17], [18].

Proposition 2 (Tangent hyperplanes for switched affine systems)**.** *Consider system* (16) *and suppose that Assumption 2 holds. Take a vector $\mathbf{M} \in \mathbb{R}^n$ such that $\mathbf{M} \geq |x_k|$ componentwise for all $k \in \mathbb{N}[0,K]$. Then*

$$\begin{aligned}
v_T(c) = \max_{x_k, z_i^k, \gamma_i^k} \; & c^\top x_{K+1} && (17a)\\
\text{s.t.} \quad & z_i^{k+1} \leq (\bar{A}_i^k x_k + \bar{b}_i^k) + \mathbf{M}(1-\gamma_i^k), && (17b)\\
& z_i^{k+1} \geq (\bar{A}_i^k x_k + \bar{b}_i^k) - \mathbf{M}(1-\gamma_i^k), && (17c)\\
& z_i^{k+1} \geq -\mathbf{M}\gamma_i^k, \quad z_i^{k+1} \leq \mathbf{M}\gamma_i^k, && (17d)\\
& z_i^k \in \mathbb{R}^n, \quad \forall k \in \mathbb{N}[1,K+1], \forall i \in \mathbb{N}[1,I], && (17e)\\
& \gamma_i^k \in \{0,1\}, \quad \forall k \in \mathbb{N}[0,K], \forall i \in \mathbb{N}[1,I], && (17f)\\
& x_k = \textstyle\sum_{i=1}^I z_i^k \in \mathbb{R}^n, \quad \forall k \in \mathbb{N}[1,K+1], && (17g)\\
& \textstyle\sum_{i=1}^I \gamma_i^k = 1, \quad \forall k \in \mathbb{N}[0,K], && (17h)\\
& x_0 \in \mathbb{R}^n \text{ assigned.} && (17i)
\end{aligned}$$

Remark 2. *The constraints (17b-d) are the big-M reformulation of the system dynamics; the continuous variables z_i^k in (17e) represent the state that one would get at step k if the system evolves from $k-1$ using the mode i multiplied by γ_i^k; the discrete variable γ_i^k in (17f) is a boolean variable taking value 1 if the system is in mode i at step k; the fact that at each step only one mode is used is encoded in (17g-h); (17i) is the initial condition.* □

Proof: To prove the statement we follow a procedure similar to the one in [27, Section IV.A]. Under Assumption 2 the switching signal $\sigma(t)$ is such that $\sigma(t) = i_k, \forall t \in [t_k, t_{k+1}), \forall k \in \mathbb{N}[0,K]$. Therefore, the finite time optimal control problem in (11) can be rewritten as

$$\begin{aligned}
v_T(c) = \max_{i_k \in \{1,\ldots,I\}} \; & c^\top x_{K+1} && (18)\\
\text{s.t.} \quad & x_{k+1} = \bar{A}_{i_k}^k x_k + \bar{b}_{i_k}^k \quad \forall k \in \mathbb{N}[0,K]\\
& x_0 \in \mathbb{R} \text{ assigned.}
\end{aligned}$$

Let us introduce the binary variables $\gamma_i^k \in \{0,1\}$ defined so that, for each $i \in \mathbb{N}[1,I]$ and $k \in \mathbb{N}[0,K]$, $\gamma_i^k = 1$ if and only if the system is in mode i in the time interval $[t_k, t_{k+1})$. Moreover, let us introduce a copy of the state vector for each possible update of the system in each possible mode: $z_i^{k+1} = (\bar{A}_i^k x_k + \bar{b}_i^k)\gamma_i^k$. Then (18) is equivalent to the following optimisation problem

$$
\begin{aligned}
v_T(c) := \max_{x_k, z_i^k, \gamma_i^k} \quad & c^\top x_{K+1} \qquad (19)\\
\text{s.t.} \quad & z_i^{k+1} = (\bar{A}_i^k x_k + \bar{b}_i^k)\gamma_i^k, \quad \forall i \in \Sigma,\\
& \textstyle\sum_{i=1}^I \gamma_i^k = 1, \quad \forall k \in \mathbb{N}[0,K],\\
& x_k = \textstyle\sum_{i=1}^I z_i^k, \quad \forall k \in \mathbb{N}[1,K+1],\\
& x_0 \in \mathbb{R} \text{ assigned.}
\end{aligned}
$$

Finally, by using the big-M method in [28, Eq. (5b)], the first equality constraint in the optimization problem (19) can be equivalently replaced by

$$
\begin{aligned}
& z_i^{k+1} \le (\bar{A}_i^k x_k + \bar{b}_i^k) + \mathbf{M}(1-\gamma_i^k), \qquad && z_i^{k+1} \ge -\mathbf{M}\gamma_i^k,\\
& z_i^{k+1} \ge (\bar{A}_i^k x_k + \bar{b}_i^k) - \mathbf{M}(1-\gamma_i^k), && z_i^{k+1} \le \mathbf{M}\gamma_i^k,
\end{aligned}
$$

leading to the equivalent reformulation given in (17). ■

We summarize our results on the hyperplane method for switched affine systems in the next corollary, which is an immediate consequence of Proposition 2 and Theorems 1, 2.

Corollary 2 (The hyperplane method for switched affine systems)**.** *Given system* (16)*, let $x_0 \in \mathbb{R}^n$ be the initial state and suppose that Assumption 2 holds. Then $\mathcal{R}_T(x_0)$ is compact. Let $v_T(c^d)$ be computed as in* (17)*. Then $\mathcal{R}_T^{out}(x_0)$ and $\mathcal{R}_T^{y,out}(x_0)$ as defined in Theorems 1 and 2 are outer approximations of $\mathcal{R}_T(x_0)$ and $\mathcal{R}_T^y(x_0)$, respectively.* □

Proof: Under Assumption 2, the reachable set $\mathcal{R}_T(x_0)$ consists of a finite number I^K of points. Each point is obtained by switching among linear systems K times. Consequently, $\mathcal{R}_T(x_0)$ is compact. The rest of the proof follows the same lines as the one of Corollary 1. The only difference among the hyperplane method for linear and switched affine systems is the method used to solve (11). ■

We note that in the case of switched affine systems there is no guarantee in general that the reachable set is convex. Consequently, as detailed in Remark 1, an inner approximation is not available and if one was to consider all possible directions, then he/she would recover exactly the *convex hull* of the projected reachable set (which is an outer approximation of the true reachable set).

C. Discussion and comparison with the literature

The main result of the previous section is the extension of the hyperplane method suggested in [16] to switched affine systems of the form given in (16). We note that the idea of describing the reachable set as the intersection of tangent half-spaces is at the core of many reachability methods based on the concept of support functions. In fact, $v_T(c)$ as we defined in equation (3) is exactly the support function of the reachable set $\mathcal{R}_T(x_0)$ evaluated for the direction c, see e.g [29]. In general, both the hyperplane method and methods based on support functions suffer from two main problems: i) for generic systems computing the support function is difficult, ii) to approximate the whole reachable set one needs a number of directions that is exponential in the system dimension. What we have shown here is that for biochemical reaction networks these two problems do not arise because: i) we showed in Proposition 2 that the burden of computing the support function for system (16) can be outsourced to an MILP solver, ii) we showed in Theorem 2 that if one is interested only in the projection of the reachable set then the number of directions needed is independent of the system dimension.

It is important to remark that efficient algorithms to tackle the problem in i) have been proposed in the literature for many different classes of systems. Specifically, [16] discusses linear systems with rectangular input constraints, [29], [30], [31] discuss the case of linear systems whose initial state and control input belong to generic convex sets, [32], [33] address linear time-varying systems, [34] discusses bilinear systems with piecewise constant inputs, while [35], [36] address hybrid systems. A toolbox based on these methods is described in [37]. None of the results above can however be applied to system (16), as we detail next.

Firstly, we note that if the switching sequence $\sigma(t)$ is fixed and known, then the switched system $\dot{x}(t) = A_{\sigma(t)}x(t) + B_{\sigma(t)}u(t)$ is actually a linear time-varying system. Therefore the set of states that such a system can reach when $u(t)$ varies in the convex control set $\mathcal{U}$ can be obtained by using [32]. Our paper however studies a different reachability problem. In fact we are interested in computing the set of states that system (16) can reach when the switching sequence $\sigma(t)$ varies in the set $\mathcal{I} = \{1, \dots, I\}$. Note that in (16) there is no control input $u(t)$ and the control action is on the switching sequence itself. Results derived for hybrid systems (e.g. in [35], [36]) cannot be applied in such a setup because therein the switching is a function of the continuous state variable and not a control variable. The closest result to ours is in [34]. Indeed, under some specific conditions on the matrices A_i and b_i, system (16) can be seen as a bilinear system. However, in [34] one cannot exploit the fact that only the projection of the reachable set is needed to tackle problem ii) above.

Secondly, we aim at constructing an approximation of the reachable set only at the final time T.[1] Instead in [29] and subsequent works the support function of $\mathcal{R}_T$ is computed by first computing the support functions of intermediate reachable sets. This idea of propagating sets of reachable states over time is at the core of many other types of reachability methods as well. These include face-lifting methods [38], [39] as well as methods propagating hyper-rectangles [40], ellipsoids [41], [42], [43], [44], polytopes [45], [46] or zonotopes [47], [48] under the assumption that the input belongs to such classes. For example, we became aware at the time of submission that the authors of [49] extended our previous works [23], [50] by suggesting the use of zonotopes. None of these works is specific for switched systems. Moreover, most of these

[1] A similar idea is used in [16], [33], [34] where the optimization problem in (11) is solved by applying Pontryagin maximum principle instead of formulating an MILP.

algorithms can only be applied for the computation of the whole reachable set. Therefore, one cannot take advantage of the fact that only a low projection of the reachable set is needed. Finally, we note that in [51] the problem of how to reconstruct the whole reachable set from two dimensional projections is discussed. This is different from our setup where instead the object of interest is the projection itself.

D. Infinite-time reachable sets

Since controlled reaction networks are typically employed in finite-time experiments, in this paper we focus on the computation of the finite-time reachable set. Nonetheless, our results could be extended for computing the infinite-time reachable set, as defined next.

Definition 3 (Infinite-time reachable set)**.** *The infinite-time reachable set from x_0 for system* (12) *is*

$$\mathcal{R}(x_0) := \{x \in \mathbb{R}^n \mid \exists T > 0 \text{ s.t. } x \in \mathcal{R}_T(x_0)\}.$$

For the case of linear systems discussed in Section III-A we refer to [23] where we prove that the method suggested in [16] is applicable also to systems with non-negative inputs.

Switched systems of the form given in (16) can be analysed over the infinite time interval $[0, +\infty)$ by imposing that the switching sequence σ satisfies the following assumption, which is the equivalent of Assumption 2 for infinite time.

Assumption 2'. *The input sequence $\sigma(t)$ can switch at most K times in $[0, +\infty)$, that is, $\sigma \in \mathcal{S}_I^\infty$*

$$\mathcal{S}_I^\infty := \{\sigma \mid \exists t_k \geq 0, \quad \forall k \in \mathbb{N}[0, K] \\ \text{s.t. } \sigma(t) = i_k \in \Sigma, \quad \forall t \in [t_k, t_{k+1})\}.$$

In fact, to compute the constant $v(c)$ of the hyperplane tangent to $\mathcal{R}(x_0)$ perpendicularly to the direction c one needs to solve the infinite-time optimal control problem

$$v(c) := \max_{x \in \mathcal{R}(x_0)} c^\top x.$$

Under Assumption 2', this problem can be solved by means of dynamic programming by adapting the "switching table procedure" proposed for infinite time quadratic optimal control problems in [27, Section V]. We leave the full derivation as future work.

IV. Controlled stochastic biochemical reaction networks

A biochemical reaction network is a system comprising S molecular species Z_1, ..., Z_S that interact through R reactions. Let $Z(t) = [Z_1(t), ..., Z_S(t)]^\top$ be the vector describing the number of molecules present in the network for each species at time t, that is, the state of the network at time t. Since each reaction r is a stochastic event [8], $Z(t)$ is a stochastic process. In the following, we always use the upper case to denote a process and the lower case to denote its realizations. For example, $z = [z_1, ..., z_S]^\top$ denotes a particular realization of the state $Z(t)$ of the stochastic process at time t.

A typical reaction $r \in \mathbb{N}[1, R]$ can be expressed as

$$\nu'_{1r} Z_1 + \ldots + \nu'_{Sr} Z_S \quad \longrightarrow \quad \nu''_{1r} Z_1 + \ldots + \nu''_{Sr} Z_S, \quad (20)$$

where $\nu'_{1r}, \ldots, \nu'_{Sr} \in \mathbb{N}$ and $\nu''_{1r}, \ldots, \nu''_{Sr} \in \mathbb{N}$ are the coefficients that determine how many molecules for each species are respectively consumed and produced by the reaction. The net effect of each reaction can thus be summarized with the *stoichiometric vector* $\nu_r \in \mathbb{N}^S$, whose components are $\nu''_{sr} - \nu'_{sr}$ for $s = 1, \ldots, S$. We say that a reaction is of order k if it involves k reactant units (i.e., $\sum_{s=1}^S \nu'_{sr} = k$) and we distinguish two classes of reactions:

-*uncontrolled* reactions that happen, in the infinitesimal interval $[t, t + dt]$, with probability

$$\alpha_r(\theta_r, z)dt := \theta_r \cdot h_r(z) \cdot dt, \quad (21)$$

where $h_r(z)$ is a given function of the available molecules z and $\theta_r \in \mathbb{R}_{\geq 0}$ is the so-called rate parameter;

- *controlled* reactions for which there exists an external signal $u_r(t)$ such that the reaction fires at time t with probability

$$u_r(t) \cdot \alpha_r(\theta_r, z)dt. \quad (22)$$

In the following we refer to $\alpha_r(\theta_r, z)$ as the propensity of the reaction and without loss of generality we assume that the controlled reactions are the first Q ones. If $h_r(z) := \Pi_{s=1}^S \binom{z_s}{\nu'_{sr}}$ we say that reaction r follows the laws of *mass action kinetics* as derived in [8]. Our analysis can however be applied to generic functions $h_r(z)$, allowing us to model different types of kinetics, such as the Michaelis-Menten [52, Section 7.3].

To illustrate the following results, we consider a model of gene expression as running example.

Example 1 (Gene expression reaction network)**.** *Consider a biochemical network consisting of two species, the mRNA (M) and the corresponding protein (P), and the following reactions*

$$\begin{array}{llll} \emptyset \xrightarrow{\alpha_1(k_r,z)} M & M \xrightarrow{\alpha_3(k_p,z)} M + P \\ M \xrightarrow{\alpha_2(\gamma_r,z)} \emptyset & P \xrightarrow{\alpha_4(\gamma_p,z)} \emptyset \end{array}$$

where the parameters k_r and k_p are the mRNA and protein production rates, while γ_r and γ_p are the mRNA and protein degradation rates, respectively. The empty set notation is used whenever a certain species is produced or degrades without involving the other species. In this context, $Z = [M, P]^\top$, $z = [m, p]^\top$, $\theta = [\theta_1, \theta_2, \theta_3, \theta_4]^\top := [k_r, \gamma_r, k_p, \gamma_p]^\top$ and the stoichiometric matrix is

$$\nu := [\nu_1, \nu_2, \nu_3, \nu_4] = \begin{bmatrix} 1 & -1 & 0 & 0 \\ 0 & 0 & 1 & -1 \end{bmatrix}.$$

In the case of mass action kinetics the propensities $\alpha_r(\theta_r, z)$ can be further specified as $\alpha_1(k_r, z) = k_r$, $\alpha_2(\gamma_r, z) = \gamma_r \cdot m$, $\alpha_3(k_p, z) = k_p \cdot m$, $\alpha_4(\gamma_p, z) = \gamma_p \cdot p$. □

Note that since the propensity of each reaction depends only on the current state of the system, the process $Z(t)$ is Markovian. Let $p(t, z) := \mathbb{P}[Z(t) = z]$ be the probability that the realization of the process Z at time t is z. Following the same procedure as in [8] one can derive a set of equations, known as *chemical master equation* (CME), describing the evolution of $p(z, t)$ as a function of the external signal $u(t)$

$$\dot{p}(z,t) = \sum_{r=1}^{Q} \left[p(z-\nu_r,t)\alpha_r(\theta_r, z-\nu_r) - p(z,t)\alpha_r(\theta_r,z)\right] u_r(t) + \sum_{r=Q+1}^{R} \left[p(z-\nu_r,t)\alpha_r(\theta_r, z-\nu_r) - p(z,t)\alpha_r(\theta_r,z)\right], \quad \forall z \in \mathbb{N}^S. \tag{23}$$

Since the previous set of equations depends on the external signal u we refer to it as the *controlled CME*. Typical biochemical reaction networks involve many different species, whose counts can theoretically grow unbounded. Consequently, the controlled CME in (23) is a system of infinitely many coupled ordinary differential equations that cannot be solved, even for very simple systems. Several analytical and computational methods have been proposed in the literature to circumvent this difficulty, see [52], [53], [54] for a comprehensive review. In the following we limit our discussion to two methods: *moment equations* [55] and *finite state projection* (FSP) [19].

A. The moment equations

We start by considering the case when all the reactions follow the laws of mass action kinetics and are at most of order one. In this case for each reaction r the propensity $h_r(z)$ is affine in the molecule counts vector z and one can show that the moments equations are closed (i.e., the dynamics of moments up to any order k do not depend on higher order moments), see for example [56]. Let $x_{\leq 2}(t)$ be a vector whose components are the moments of $Z(t)$ up to second order. From [56, Equations (6) and (7)] one gets

$$\dot{x}_{\leq 2}(t) = A(u(t))x_{\leq 2}(t) + b(u(t)). \tag{24}$$

Example 2. *Consider the gene expression model of Example 1. Assume that the reactions follow the mass action kinetics and that an external input signal influencing the first reaction, that is the mRNA production, is available (as in [1], [2], [3], [4], [5]), so that $\alpha_1(k_r, z) := k_r \cdot u(t)$. Set*[2]

$$x_{\leq 2} := [\mathbb{E}[M], \mathbb{E}[P], \mathbb{V}[M,P], \mathbb{V}[P]]^\top.$$

Then the moments evolution over time is expressed as

$$\dot{x}_{\leq 2}(t) = Ax_{\leq 2}(t) + Bu(t), \tag{25}$$

where

$$A = \begin{bmatrix} -\gamma_r & 0 & 0 & 0 \\ k_p & -\gamma_p & 0 & 0 \\ k_p & 0 & -(\gamma_r+\gamma_p) & 0 \\ k_p & \gamma_p & 2k_p & -2\gamma_p \end{bmatrix}, \quad B = \begin{bmatrix} k_r \\ 0 \\ 0 \\ 0 \end{bmatrix}.$$

□

Since the input $u(t)$ may appear in the entries of the A matrix, the moment equations (24) are in general nonlinear. To overcome this issue we introduce the following assumption on the external signal $u(t)$.

Assumption 3. *The external signal $u(t)$ can switch at most K times within the set Σ^d, as defined in Assumption 1, at preassigned switching instants $0 = t_0 < \ldots < t_{K+1} = T$.*

Assumption 3 imposes that the number of switchings and their timing during a given experiment is fixed a priori. This assumption can be motivated by the fact that changes in the external stimulus are costly and/or stressful for the cells. Moreover, it is trivially satisfied if the stimulus can only be changed simultaneously with some fixed events, such as culture dilution or measurements. The great advantage of Assumption 3 is that, as illustrated in the following remark, it allows us to rewrite the nonlinear moment equations (24) as a switched affine system so that the theoretical tools described in Section III-B can be applied.

Remark 3. *The set Σ^d has finite cardinality $I := \Pi_{r=1}^{Q} q_r$ and we can enumerate its elements as $u^i, i \in \mathbb{N}[1,I]$. Set $A_i := A(u^i)$ and $b_i := b(u^i)$, for all $i \in \mathbb{N}[1,I]$. For any fixed external signal $u(t)$ satisfying Assumption 3 we can construct a sequence of indices in $\mathbb{N}[1,I]$ such that, at any time t, $\sigma(t) = i$ if and only if $u(t) = u^i$, so that system* (24) *can be equivalently rewritten as $\dot{x}_{\leq 2}(t) = A_{\sigma(t)}x_{\leq 2}(t) + b_{\sigma(t)}$. Note that the switching sequence σ satisfies Assumption 2.* □

B. The finite state projection

Let us introduce a total ordering $\{z^j\}_{j=1}^{\infty}$ in the set of all possible state realizations $z \in \mathbb{N}^S$. For the system in Example 1, we could for instance use the mapping

$$z^1 = (0,0),\ z^2 = (1,0),\ z^3 = (0,1),\ z^4 = (2,0),$$
$$z^5 = (1,1),\ z^6 = (0,2),\ z^7 = (3,0),\ z^8 = (2,1),\ \ldots$$

where (m,p) denotes the state with m mRNA copies and p proteins (see Fig. 2).

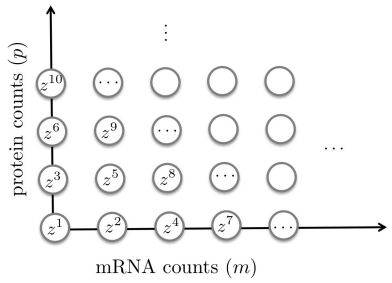

Fig. 2. State space for the gene expression system of Example 1.

Following the same steps as in [19] and setting[3] $P_j(t) := p(z^j, t)$, the *controlled* CME in (23) can be rewritten as the nonlinear infinite dimensional system

$$\dot{P}(t) = F(u(t))P(t), \tag{26}$$

where $P(t)$ is an infinite dimensional vector with entries in $[0,1]$. If the signal $u(t)$ satisfies Assumption 3, then (26) can be rewritten as an infinite dimensional linear switched system

$$\dot{P}(t) = F_{\sigma(t)}P(t), \tag{27}$$

with switching signal $\sigma(t)$ constructed from $u(t)$ as detailed in Remark 3, $I = \Pi_{r=1}^{Q} q_r$ modes and matrices $F_i := F(u^i)$. Note that system (27) can also be thought of as a Markov

[2]The mRNA follows a birth-death process hence $\mathbb{E}[M] = \mathbb{V}[M]$ [50].

[3]Not to be confused with the symbol used to denote the amount of protein.

chain with countably many states $z^j \in \mathbb{N}^S$ and time-varying transition matrix $F_{\sigma(t)}$.

As in the FSP method for the uncontrolled CME [19], one can try to approximate the behavior of the infinite Markov chain in (27) by constructing a reduced Markov chain that keeps track of the probability of visiting only the states indexed in a suitable set J. To this end, let us define the reduced order system

$$\dot{\bar{P}}_J(t) = \left[F_{\sigma(t)}\right]_J \bar{P}_J(t), \quad \bar{P}_J(0) = P_J(0), \tag{28}$$

where $P_J(0)$ is the subvector of $P(0)$ corresponding to the indices in J, and $[F]_J$ denotes the submatrix of F obtained by selecting only the rows and columns with indices in J. Note that while the full matrix $F_{\sigma(t)}$ is stochastic, the reduced matrix $\left[F_{\sigma(t)}\right]_J$ is substochastic. Consequently, the probability mass is in general not preserved in (28) (i.e. $\mathbb{1}^\top \bar{P}_J(t)$ may decrease with time). From now on, we denote by $P(T;\sigma)$ and $\bar{P}_J(T;\sigma)$ the solutions at time T of system (27) and system (28), respectively, when the switching signal σ is applied. The dependence on the initial conditions $P(0)$ and $P_J(0)$ is omitted to keep the notation compact. As in the uncontrolled case, the truncated system (28) is a good approximation of the original system (27) if most of the probability mass lies in J. However in the controlled case we need to guarantee that this happens for all possible switching signals. This intuition is formalized in the following assumption.

Assumption 4. *For a given finite set of state indices J, an initial condition $P_J(0)$, a given tolerance $\varepsilon > 0$ and a finite instant $T > 0$,*

$$\mathbb{1}^\top \bar{P}_J(T;\sigma) \geq 1 - \varepsilon, \quad \forall \sigma \in \mathcal{S}_I^K. \tag{29}$$

Remark 4. *Our subsequent results rely on the assumption that a set J satisfying Assumption 4 is available. We note that:*
i) For a given candidate set J one can find the smallest $\varepsilon > 0$ such that the pair (J, ε) satisfies Assumption 4 by solving an MILP. In fact Assumption 4 holds if and only if

$$1 - \varepsilon \leq \min_{\sigma \in \mathcal{S}_I^K} \quad \mathbb{1}^\top \bar{P}_J(T;\sigma)$$
$$\text{s.t. } \dot{\bar{P}}_J(t;\sigma) = \left[F_{\sigma(t)}\right]_J \bar{P}_J(t;\sigma), \ \bar{P}_J(0) = P_J(0).$$

This problem has the same structure as (11)*. Therefore, as illustrated in Section III-B, Assumption 4 can be checked by solving the MILP* (17) *for the switched affine system* (28) *by setting $c = \mathbb{1}$ and $\mathbf{M} = \mathbb{1}$.*
ii) Finding a good candidate set is usually a recursive procedure, where one starts with a candidate set J_1 (possibly selected by running a small number of stochastic simulations) and computes the corresponding error ε_1, as in i). If this is larger than the desired error ε, then a second candidate set J_2 can be obtained by enlarging J_1 to include more states and so on.
iii) Depending on the network it might not always be possible to find a set J such that Assumption 4 is met for the desired T and precision ε, e.g. Assumption 4 cannot be met if the moments blow up in finite-time. Conditions guaranteeing that this is not the case have been discussed in [57], [58], [59]. □

Under Assumption 4, the following relation between the solutions of (27) and (28) holds.

Proposition 3 (FSP for controlled CME)**.** *If Assumptions 2 and 4 hold, then for every switching signal $\sigma \in \mathcal{S}_I^K$, it holds*

$$P_j(T;\sigma) \geq \bar{P}_j(T;\sigma), \quad \forall j \in J$$
$$\|P_J(T;\sigma) - \bar{P}_J(T;\sigma)\|_1 \leq \varepsilon.$$

Proof: This result has been proven in [19] for linear systems. We extend it here to the case of switched systems with K switchings. Note that for any $i \in \mathbb{N}[1, I]$, $F_i := F(u^i)$ has non-negative off diagonal elements [19]. Hence, using the same argument as in [19, Theorem 2.1] it can be shown that for any index set J, and any $\tau \geq 0$

$$[\exp(F_i \tau)]_J \geq \exp([F_i]_J \tau) \geq 0, \quad \forall i \in 1, \ldots, I.$$

Consider an arbitrary switching signal $\sigma \in \mathcal{S}_I^K$. We have

$$\begin{aligned} P_J(T;\sigma) &= [\Pi_{k=0}^K \exp(F_{i_k}(t_{k+1} - t_k)) \cdot P(0)]_J \\ &\geq \Pi_{k=0}^K [\exp(F_{i_k}(t_{k+1} - t_k))]_J \cdot P_J(0) \\ &\geq \Pi_{k=0}^K \exp([F_{i_k}]_J (t_{k+1} - t_k)) \cdot P_J(0) = \bar{P}_J(T;\sigma). \end{aligned} \tag{30}$$

Moreover, from $1 = \sum_{j=1}^\infty P_j(T;\sigma) \geq \sum_{j \in J} P_j(T;\sigma) = \mathbb{1}^\top P_J(T;\sigma)$ and Assumption 4, we get

$$\mathbb{1}^\top \bar{P}_J(T;\sigma) \geq 1 - \varepsilon \geq \mathbb{1}^\top P_J(T;\sigma) - \varepsilon. \tag{31}$$

Combining (30) and (31) yields $0 \leq \mathbb{1}^\top P_J(T;\sigma) - \mathbb{1}^\top \bar{P}_J(T;\sigma) \leq \varepsilon$, thus $\|P_J(T;\sigma) - \bar{P}_J(T;\sigma)\|_1 \leq \varepsilon$. ■

V. Analysis of the reachable set

We here show how the reachability tools of Sections II and III can be applied to the moment equation and FSP reformulations derived in Sections IV-A and IV-B, under different assumptions. Fig. 3 presents a conceptual scheme of this section.

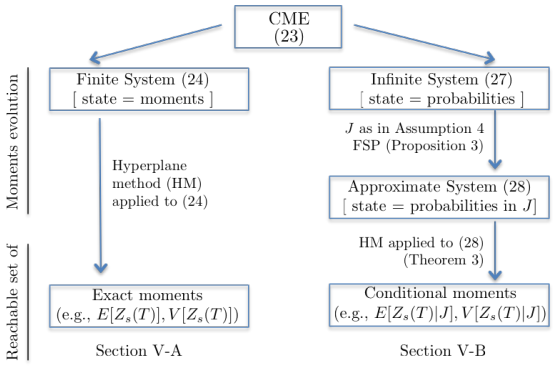

Fig. 3. Conceptual scheme for the reachable set analysis of biochemical networks.

A. Reachable set of networks with affine propensities via moment equations

The methods developed in Sections II and III can be applied to the moments equations in (24) to approximate the desired projected reachable set. To illustrate the proposed procedure, we distinguish two cases depending on whether the external signal $u(t)$ influences reactions of order zero or one.

1) Linear moments equations: We start by considering the case when all and only the reactions of order zero are controlled, so that $h_r(z) = 1$ for $r \in \mathbb{N}[1, Q]$ and $h_r(z) = {\nu'_r}^\top z$ for $r \in \mathbb{N}[Q+1, R]$. This is the simplest scenario since the system of moment equations given in (24) becomes linear

$$\dot{x}_{\leq 2}(t) = Ax_{\leq 2}(t) + Bu(t), \tag{32}$$

see [56, Equations (6) and (7)]. Consequently, the theoretical results of Section III-A can be applied to (32) by setting $\sigma(t) \equiv u(t)$. If the external signal $u \equiv \sigma$ satisfies Assumption 1, both inner and outer approximations of the reachable set can be computed by using Corollary 1.

2) Switched affine moments equations: Under Assumption 3, (24) can be equivalently rewritten as a switched affine system, as described in Remark 3. Consequently, the theoretical results of Section III-B can be applied and an outer approximation of the reachable set can be computed by using Corollary 2.

B. Reachable set of networks with generic propensities via finite state projection

If the network contains reactions of order higher than one or if the reactions do not follow the laws of mass action kinetics, then $h_r(z)$ might be non-affine. In such cases, the arguments illustrated in the previous subsection cannot be applied. We here show how the FSP approximation of the CME derived in Section IV-B can be used to overcome this problem.

Firstly note that, from system (27), one can compute the evolution of the *uncentered* moments of $Z(t)$, as a linear function of $P(t)$. [4] For example, if we let z_s^j be the amount of species Z_s in the state z^j, then the mean $\mathbb{E}[Z_s]$ of any species s can be obtained as $l^\top P(t)$, by setting $l := \left[z_s^1,\ z_s^2,\ \dots\right]^\top$, and the second uncentered moment $\mathbb{E}[Z_s^2]$ can be obtained as $l^\top P(t)$, by setting $l := \left[(z_s^1)^2,\ (z_s^2)^2,\ \dots\right]^\top$. Consequently the desired projected reachable set coincides with the output reachable set of the infinite dimensional linear switched system (27) with linear output

$$y(t) = \left[l^1,\ \ l^2\right]^\top P(t), \tag{33}$$

where l^1 and l^2 are the infinite vectors associated with any desired pair of moments. Note that l^1 and l^2 are non-negative.

Example 1 (cont.) *With the ordering introduced at the beginning of the section, the uncentered protein moments up to order two can be computed as the output of* (27) *by setting*

$$\begin{aligned} l^1 &= \left[\begin{array}{cccccccccc} 0 & 0 & 1 & 0 & 1 & 2 & 0 & 1 & \dots \end{array}\right]^\top, \\ l^2 &= \left[\begin{array}{cccccccccc} 0 & 0 & 1 & 0 & 1 & 4 & 0 & 1 & \dots \end{array}\right]^\top. \end{aligned} \tag{34}$$

Let l_j^1 and l_j^2 be the j-th components of the vectors l^1 and l^2, respectively, as defined in (33). For a given species of interest s and set J, we denote by

$$y_1(t;\sigma) := \frac{\sum_{j\in J} l_j^1 \cdot P_j(t;\sigma)}{\sum_{j\in J} P_j(t;\sigma)},\ y_2(t;\sigma) := \frac{\sum_{j\in J} l_j^2 \cdot P_j(t;\sigma)}{\sum_{j\in J} P_j(t;\sigma)} \tag{35}$$

[4] The reachable set for the *centered* moments can be immediately computed from the reachable set of the *uncentered* ones, since there is a bijective relation between the set of *centered* and *uncentered* moments up to any desired order.

the moments associated with l^1 and l^2 *conditioned on the fact that* $Z(t)$ *is in* J *and the switching signal* σ *is applied*. For example if one is interested in the mean and second order moment of a specific species $Z_s(t)$ we get $y_1(t;\sigma) = \mathbb{E}\left[Z_s(t) \mid Z(t) \in J, \sigma(\cdot)\right]$ and $y_2(t;\sigma) = \mathbb{E}\left[Z_s^2(t) \mid Z(t) \in J, \sigma(\cdot)\right]$. The aim of this section is to obtain an outer approximation of the output reachable set of the infinite system (27) with the nonlinear output (35), by using computations involving only the finite dimensional system (28). To this end, we define the two entries of the output of the finite dimensional system as

$$\begin{aligned} \bar{y}_1(t;\sigma) &:= \textstyle\sum_{j\in J} l_j^1 \cdot \bar{P}_j(t;\sigma) =: (\bar{l}^1)^\top \bar{P}_J(t;\sigma) \\ \bar{y}_2(t;\sigma) &:= \textstyle\sum_{j\in J} l_j^2 \cdot \bar{P}_j(t;\sigma) =: (\bar{l}^2)^\top \bar{P}_J(t;\sigma). \end{aligned} \tag{36}$$

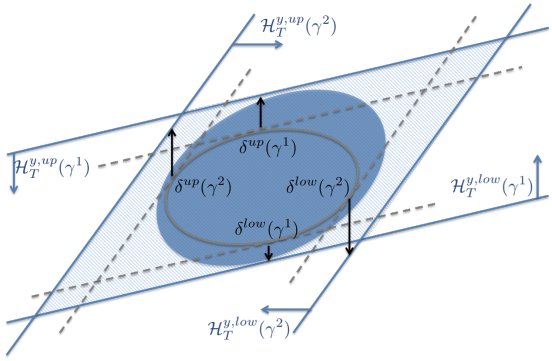

Fig. 4. Illustration of Theorem 3. The inner grey circle is the reachable set of the finite dimentional system (28). The dotted grey lines are hyperplanes tangent to such set. The solid blue lines are obtained by translating such hyperplanes by the constants $\delta^{up}(\gamma^d)$ and $\delta^{low}(\gamma^d)$, as computed in Theorem 3, for the upper and lower bounds respectively. The reachable set of the original system (27) is the blue area, which is correctly contained in the intersection of the translated hyperspaces (lined region).

The main idea is that the hyperplanes tangent to the reachable set of the finite system (28) with output (36) can be computed using the techniques of Section III. In the next theorem we show that it is possible to translate such hyperplanes, by suitable constants $\delta^{up}(\gamma^d), \delta^{low}(\gamma^d)$, to guarantee that the reachable set of the original infinite system (27) with the nonlinear output (35) is contained in the intersection of the translated hyperplanes, as illustrated in Figure 4.

Theorem 3. *Suppose Assumptions 3 and 4 hold. Let* $\mathcal{R}_T^y(x_0)$ *be the output reachable set at time* $T > 0$ *of system* (27) *with output* (35). *Choose* D *values* $\gamma^d \in \mathbb{R}$ *and set* $c^d := (\bar{l}^2) - \gamma^d(\bar{l}^1) \in \mathbb{R}^n$, *with* $\bar{l}^1, \bar{l}^2$ *as in* (36). *Set*

$$\begin{aligned} \mathcal{H}_T^{y,up}(\gamma^d) &:= \{w \in \mathbb{R}^2 \mid w_2 \leq \gamma^d w_1 + \bar{v}_T(c^d) + \delta^{up}(\gamma^d)\}, \\ \mathcal{H}_T^{y,low}(\gamma^d) &:= \{w \in \mathbb{R}^2 \mid w_2 \geq \gamma^d w_1 - \bar{v}_T(-c^d) - \delta^{low}(\gamma^d)\}, \end{aligned}$$

where $\bar{v}_T(c^d)$ *is the constant that makes the hyperplane* $\mathrm{H}_T(c^d)$ *in* (5) *tangent to the reachable set of the finite system* (28) *(i.e.* $\bar{v}_T(c^d)$ *can be computed as in* (17)*) and*

$$\begin{aligned} \delta^{up}(\gamma^d) &:= \tfrac{2\varepsilon}{1-\varepsilon} \cdot (\max\{0, -\gamma^d\} \cdot \|\bar{l}^1\|_\infty + \|\bar{l}^2\|_\infty), \\ \delta^{low}(\gamma^d) &:= \tfrac{2\varepsilon}{1-\varepsilon} \cdot (\max\{0, \gamma^d\} \cdot \|\bar{l}^1\|_\infty), \end{aligned}$$

with ε *as in Assumption 4. Then the set*

$$\mathcal{R}_T^{y,out}(x_0) := \cap_{d=1}^D \{\mathcal{H}_T^{y,up}(\gamma^d) \cap \mathcal{H}_T^{y,low}(\gamma^d)\}$$

is an outer approximation of $\mathcal{R}_T^y(x_0)$. □

Proof: Firstly note that if the external signal u satisfies Assumption 3 then the corresponding switching signal $\sigma(t)$ (constructed as in Remark 3) satisfies Assumption 2. Let $\bar{\mathcal{R}}_T^y(x_0)$ be the output reachable set of the finite dimensional system (28) with output (36). Proposition 2 guarantees that for any direction c^d the constants $\bar{v}_T(c^d)$ and $\bar{v}_T(-c^d)$ that make

$$\bar{\mathcal{H}}_T^{y,up}(\gamma^d) := \{w \in \mathbb{R}^2 \mid w_2 \leq \gamma^d w_1 + \bar{v}_T(c^d)\}$$
$$\bar{\mathcal{H}}_T^{y,low}(\gamma^d) := \{w \in \mathbb{R}^2 \mid w_2 \geq \gamma^d w_1 - \bar{v}_T(-c^d)\}$$

tangent to $\bar{\mathcal{R}}_T^y(x_0)$ can be computed by solving the MILP (17) for system (28). The main idea of the proof is to show that if we shift the halfspaces $\bar{\mathcal{H}}_T^{y,up}(\gamma^d), \bar{\mathcal{H}}_T^{y,low}(\gamma^d)$ by suitably defined constants $\delta^{up}(\gamma^d), \delta^{low}(\gamma^d)$ we can guarantee that the original reachable set $\mathcal{R}_T^y(x_0)$ is a subset of the shifted halfspaces $\mathcal{H}_T^{y,up}(\gamma^d), \mathcal{H}_T^{y,low}(\gamma^d)$ defined in the statement. The result then follows since $\mathcal{R}_T^{y,out}(x_0)$ is defined as the intersection of hyperspaces containing $\mathcal{R}_T^y(x_0)$.

We show how to derive the constant $\delta^{up}(\gamma^d)$, the derivation of $\delta^{low}(\gamma^d)$ is similar. To this end, we start by focusing on the first component of the output and for simplicity we will omit the dependence on $(T;\sigma)$ in $P_j, \bar{P}_j, y$ and $\bar{y}$. Take any switching signal $\sigma \in \mathcal{S}_I^K$. By taking into account the following conditions: (1) $l_j^1 \geq 0$ for all $j \in J$; (2) $P_j \geq \bar{P}_j$ for all $j \in J$, due to Proposition 3, and (3) $\sum_{j\in J} P_j \leq 1$, we get $y_1 \geq \bar{y}_1$. Consequently, at time $t = T$ we have

$$\begin{aligned}
|y_1 - \bar{y}_1| = y_1 - \bar{y}_1 &= \tfrac{\sum_{j\in J} l_j^1 \cdot P_j}{\sum_{j\in J} P_j} - \textstyle\sum_{j\in J} l_j^1 \cdot \bar{P}_j \\
&\leq \tfrac{\sum_{j\in J} l_j^1 \cdot P_j}{1-\varepsilon} - \textstyle\sum_{j\in J} l_j^1 \cdot \bar{P}_j \\
&= \left(1 + \tfrac{\varepsilon}{1-\varepsilon}\right) \textstyle\sum_{j\in J} l_j^1 \cdot P_j - \sum_{j\in J} l_j^1 \cdot \bar{P}_j \\
&= \tfrac{\varepsilon}{1-\varepsilon} \textstyle\sum_{j\in J} l_j^1 \cdot P_j + \sum_{j\in J} l_j^1 \cdot (P_j - \bar{P}_j) \\
&\leq \|\bar{l}^1\|_\infty \left(\tfrac{\varepsilon}{1-\varepsilon} \textstyle\sum_{j\in J} P_j + \sum_{j\in J} (P_j - \bar{P}_j)\right) \\
&\leq \|\bar{l}^1\|_\infty \left(\tfrac{\varepsilon}{1-\varepsilon} + \|P_J - \bar{P}_J\|_1\right) \leq \|\bar{l}^1\|_\infty \tfrac{2\varepsilon}{1-\varepsilon},
\end{aligned}$$

where we used $\sum_{j\in J} P_j \geq \sum_{j\in J} \bar{P}_j \geq 1 - \varepsilon$ (due to Assumption 4), and $P_j \geq \bar{P}_j, \|P_J - \bar{P}_J\|_1 \leq \varepsilon$ (following from Proposition 3). To summarize, $\bar{y}_1 \leq y_1 \leq \bar{y}_1 + \|\bar{l}^1\|_\infty \frac{2\varepsilon}{1-\varepsilon}$. Similarly, it can be proven that $\bar{y}_2 \leq y_2 \leq \bar{y}_2 + \|\bar{l}^2\|_\infty \frac{2\varepsilon}{1-\varepsilon}$. Consider any pair $(y_1, y_2) \in \mathcal{R}_T^y(x_0)$ and the associated pair $(\bar{y}_1, \bar{y}_2) \in \bar{\mathcal{R}}_T^y(x_0)$ (i.e. the two output pairs obtained from (27) and (28) when the same σ is applied). Note that $(\bar{y}_1, \bar{y}_2) \in \bar{\mathcal{R}}_T^y(x_0)$ implies $(\bar{y}_1, \bar{y}_2) \in \bar{\mathcal{H}}_T^y(\gamma^d)$ for any γ^d. The previous relations then imply that if $\gamma^d \geq 0$,

$$\begin{aligned}
y_2 &\leq \bar{y}_2 + \|\bar{l}^2\|_\infty \tfrac{2\varepsilon}{1-\varepsilon} \leq \gamma^d \bar{y}_1 + \bar{v}_T(c^d) + \|\bar{l}^2\|_\infty \tfrac{2\varepsilon}{1-\varepsilon} \\
&\leq \gamma^d y_1 + \bar{v}_T(c^d) + \|\bar{l}^2\|_\infty \tfrac{2\varepsilon}{1-\varepsilon} = \gamma^d y_1 + \bar{v}_T(c^d) + \delta^{up}(\gamma^d).
\end{aligned}$$

On the other hand, when $\gamma^d < 0$

$$\begin{aligned}
y_2 &\leq \bar{y}_2 + \|\bar{l}^2\|_\infty \tfrac{2\varepsilon}{1-\varepsilon} \leq \gamma^d \bar{y}_1 + \bar{v}_T(c^d) + \|\bar{l}^2\|_\infty \tfrac{2\varepsilon}{1-\varepsilon} \\
&\leq \gamma^d y_1 + \bar{v}_T(c^d) + (\|\bar{l}^2\|_\infty - \gamma^d \|\bar{l}^1\|_\infty) \tfrac{2\varepsilon}{1-\varepsilon} \\
&= \gamma^d y_1 + \bar{v}_T(c^d) + \delta^{up}(\gamma^d).
\end{aligned}$$

Therefore for every signal σ and every γ^d it holds $y_2(T;\sigma) \leq \gamma^d y_1(T;\sigma) + \bar{v}_T(c^d) + \delta^{up}(\gamma^d)$ and consequently $[y_1(T;\sigma), y_2(T;\sigma)]^\top \in \mathcal{H}_T^{y,up}(\gamma^d)$. ■

VI. Analysis of single cell realizations

The previous analysis focused on characterising what combinations of moments of the stochastic biochemical reaction network are achievable by using the available external input. In this section, we change perspective and instead of looking at population properties we focus on single cell trajectories. Specifically, we are interested in characterising the probability that a single realization of the stochastic process will satisfy a specific property at the final time T (e.g. the number of copies of a certain species is higher/lower than a certain threshold) when starting from an initial condition $P(0)$. Note that we can start either deterministically from a given state z^i (by setting $P(0) = e_i$) or stochastically from any state according to a generic vector of probabilities $P(0)$. To define the problem let us call $\mathcal{T}$ the target set, that is, the set of all indices i associated with a state z^i in the Markov chain (26) that satisfies the desired property. Note that this set might be of infinite size. We restrict our analysis to external signals satisfying Assumption 3, so that we can map the external signal u to the switching signal σ, as detailed in Remark 3. For a fixed signal σ the solution of (27) immediately allows one to compute the probability that the state at time T belongs to $\mathcal{T}$, and thus has the desired property, as $\mathcal{P}_\mathcal{T}(\sigma) := \mathbb{1}_\mathcal{T}^\top P(T;\sigma)$ where $\mathbb{1}_\mathcal{T}$ is an infinite vector that has the ith component equal to 1 if $i \in \mathcal{T}$ and 0 otherwise. Our objective is to select the switching signal $\sigma(t)$ (and thus the external signal $u(t)$) that maximizes the probability $\mathcal{P}_\mathcal{T}(\sigma)$.[5] That is, we aim at solving

$$\mathcal{P}_\mathcal{T}^\star := \max_{\sigma\in\mathcal{S}_I^K} \mathcal{P}_\mathcal{T}(\sigma), \qquad \sigma^\star := \arg\max_{\sigma\in\mathcal{S}_I^K} \mathcal{P}_\mathcal{T}(\sigma), \quad (37)$$

where I is the cardinality of Σ^d as by Remark 3. Note that $\mathcal{P}_\mathcal{T}(\sigma)$ in (37) is computed according to $P(T;\sigma)$ which is an infinite dimentional vector. In the next theorem we show how to overcome this issue and approximately solve (37) by using the FSP approach of Proposition 3 and the reformulation as MILP given in Proposition 2. To this end, let

$$\bar{\sigma}^\star := \arg\max_{\sigma\in\mathcal{S}_I^K} \bar{\mathcal{P}}_\mathcal{T}(\sigma). \quad (38)$$

where $\bar{\mathcal{P}}_\mathcal{T}(\sigma) := \bar{\mathbb{1}}_\mathcal{T}^\top \bar{P}_J(T;\sigma)$ is the probability that the final state of the *reduced* Markov chain (28) belongs to $\mathcal{T} \cap J$ at time T given the switching signal σ, and $\bar{\mathbb{1}}_\mathcal{T}$ is a vector of size $|J|$ that has 1 in the positions corresponding to states of J that belong also to $\mathcal{T}$, and 0 otherwise.

Theorem 4. *Suppose that Assumptions 3 and 4 hold. Then*

$$\mathcal{P}_\mathcal{T}(\bar{\sigma}^\star) \geq \mathcal{P}_\mathcal{T}^\star - 2\varepsilon.$$

Moreover (38) *can be solved by solving the MILP in* (17) *for system* (28) *with* $c = \bar{\mathbb{1}}_\mathcal{T}$ *and* $\mathbf{M} = \mathbb{1}$. □

Proof: Under Assumption 3 and 4, for any set $\mathcal{T}$ and any signal σ, we get

$$\begin{aligned}
\mathbb{1}_\mathcal{T}^\top P &= \textstyle\sum_{i\in\mathcal{T}} P_i \leq \sum_{i\in\mathcal{T}\cap J} P_i + \sum_{i\notin J} P_i \leq \sum_{i\in\mathcal{T}\cap J} P_i + \varepsilon \\
&\leq \textstyle\sum_{i\in\mathcal{T}\cap J} \bar{P}_i + \sum_{i\in\mathcal{T}\cap J} |P_i - \bar{P}_i| + \varepsilon \\
&\leq \textstyle\sum_{i\in\mathcal{T}\cap J} \bar{P}_i + \|P_J - \bar{P}_J\|_1 + \varepsilon = \bar{\mathbb{1}}_\mathcal{T}^\top \bar{P} + 2\varepsilon,
\end{aligned}$$

[5] Note that one can use the same tools to maximize the probability of *avoiding* a given set $\mathcal{D}$ by maximizing the probability of being in $\mathcal{T} = \mathcal{D}^c$.

and $\mathbb{1}_{\mathcal{T}}^{\top} P = \sum_{i\in\mathcal{T}} P_i \geq \sum_{i\in\mathcal{T}\cap J} P_i \geq \sum_{i\in\mathcal{T}\cap J} \bar{P}_i = \bar{\mathbb{1}}_{\mathcal{T}}^{\top} \bar{P}$, where we used Assumption 4 and Proposition 3 and we omitted $(T;\sigma)$ for simplicity. To sum up, for each σ,

$$\bar{\mathcal{P}}_{\mathcal{T}}(\sigma) \leq \mathcal{P}_{\mathcal{T}}(\sigma) \leq \bar{\mathcal{P}}_{\mathcal{T}}(\sigma) + 2\varepsilon.$$

By imposing $\sigma = \sigma^\star$ we get $\mathcal{P}_{\mathcal{T}}^\star = \mathcal{P}_{\mathcal{T}}(\sigma^\star) \leq \bar{\mathcal{P}}_{\mathcal{T}}(\sigma^\star) + 2\varepsilon \leq \bar{\mathcal{P}}_{\mathcal{T}}(\bar{\sigma}^\star) + 2\varepsilon$. By imposing $\sigma = \bar{\sigma}^\star$ we get $\bar{\mathcal{P}}_{\mathcal{T}}(\bar{\sigma}^\star) \leq \mathcal{P}_{\mathcal{T}}(\bar{\sigma}^\star)$. Combining the last two inequalities we get the desired bound. The last result can be proven as in Proposition 2. Note that $\bar{P}$ is a vector of probabilities, hence we can set $\mathbf{M} = \mathbb{1}$. ■

VII. The Gene Expression Network Case Study

To illustrate our method we consider again the gene expression model of Example 1 and determine what combinations of the protein mean and variance are achievable starting from the zero state, under different assumptions on the external signal. The following examples cover a wide range of difficulties typically encountered in the analysis of stochastic biochemical reaction networks. In Section VII.A we study networks with mass action kinetics of order at most one leading to *closed moment equations* so that one can use the tools of Section V-A. Specifically, in Section VII.A1 only zero order reactions are controlled, leading to linear moment equations; in Sections VII.A2 and VII.A3 we assume that the external signal influences also a first order reaction, leading to a switched system. In Section VII.B we study systems with *non-closed moment equations* so that one needs to use the tools of Section V-B. Specifically, in Sections VII.B1 and VII.B2 we consider two different types of non-linearities which are Michaelis-Menten and bimolecular reactions, respectively.

For all the reachable set computations we use $D = 11$. The overall computation time is therefore the time needed to solve (11) times $2D$ (for each direction one needs to compute both c^d and $-c^d$)). As proven in Proposition 1, for linear systems problem (11) can be solved by evaluating (14). For switched systems, as proven in Proposition 2, problem (11) can be solved by solving the MILP in (17). For each case study, we report the average time needed to solve such MILPs by using Gurobi 7.5.1 [60] and Matlab R2016b on a notebook computer running Mac OS X 10.11.6 (CPU: 2.4 GHz Intel Core i5, Memory: 8 GB 1600 MHz DDR3). When possible we compare our method with the toolbox CORA [61].[6]

A. Closed moment equations

1) Single input: Consider the gene expression model with one external signal and reactions following the mass action kinetics, as described in Example 2. In this case, the moments equations are linear and the protein mean and variance can be obtained by setting $L := [e_2, e_4]^\top$ as output matrix for the linear system (25). Depending on the experimental setup, the external signal $u(t)$ may take values in the set $\Sigma^d := \{0, 1\}$, if the input is of the ON-OFF type [1], [2], [3], [5], or in the interval $\Sigma^c := [0, 1]$, if the input is continuous [4]. Corollary 1 guarantees the validity of the following results both for Σ^d and Σ^c. The problem of computing an outer approximation of the reachable set of this system was studied in [50] using ad hoc methods. In Fig. 5a) we compare the outer approximation obtained therein (magenta dashed/dotted line) with the inner (solid red) and outer (dashed blue) approximations that we obtained using the methods for linear moment equations of Section V-A1. For Fig. 5, we used the parameters $k_r = 0.0236, \gamma_r = 0.0503, k_p = 0.18, \gamma_p = 0.0121$ (all in units of min^{-1}) and set $T = 360$ min. Fig. 5a) shows that the outer approximation computed using the hyperplane method is more accurate than the one previously obtained in [50]. Moreover, since inner and outer approximations practically coincide, this method allows one to effectively recover the reachable set. The grey area in Fig. 5a) illustrates the reachable set computed with the function 'linearSys' of the CORA toolbox with the settings timeStep=1, taylorTerms=4, zonotopeOrder=200, which were selected to minimise the computation time while maintaining the same accuracy as the method in Section V-A1. The simulation time for the method of Section V-A1 is 3.1350 and for CORA is 3.3183 seconds.

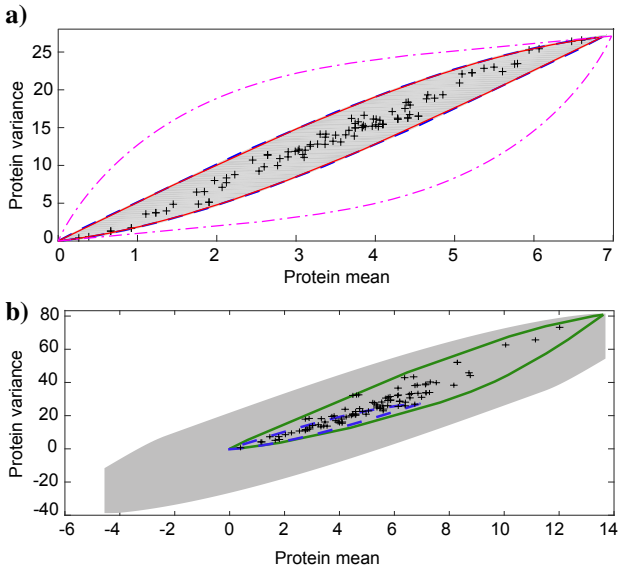

Fig. 5. *Figure a) [One external signal]:* Comparison of i) the inner (red solid) and outer (blue dashed) approximations of the reachable set for the protein mean and variance, according to model (25), computed using the hyperplane method, ii) the outer approximation computed according to [50] (magenta dashed/dotted) and iii) the outer approximation computed using CORA (grey area). The black crosses represent the output for 100 random inputs. *Figure b) [Two external signals]:* Comparison of the outer approximations of the reachable set with two inputs obtained using the hyperplane method (green solid) and CORA (grey area). The blue dashed line is the reachable set for one external signal as in part a).

2) Two inputs: Consider again Example 1, but now assume that both the mRNA production and degradation can be controlled, so that the vector of propensities is $\alpha(z) = [k_r{\cdot}u_1(t),\ \gamma_r{\cdot}m{\cdot}u_2(t),\ k_p{\cdot}m,\ \gamma_p{\cdot}p]^\top$ and $u(t) := \begin{bmatrix} u_1(t) \\ u_2(t) \end{bmatrix}$, as studied in [9]. Note that in this case $u_2(t)$ affects the A matrix in (24) and consequently the system of moment equations is nonlinear. We therefore assume that switchings can occur

[6] We note that, contrary to our method that only depends on the parameter D, the performance of CORA depends on a number of settings, leading to a trade off between simulation time and accuracy. We tested a number of different combinations and we report here the most accurate result that we could achieve. In all the cases we set reductionTechnique='girard'. For the simulations of Section VII.B the amount of memory required by CORA surpassed the available memory.

every 30 min, so that Assumption 3 is satisfied with $K = 12$ and use the hyperplane method as described in Section V-A2 with input set

$$\Sigma^{\text{2in}} := \left\{ \begin{bmatrix} 0 \\ 1 \end{bmatrix}, \begin{bmatrix} 0 \\ 0.5 \end{bmatrix}, \begin{bmatrix} 1 \\ 1 \end{bmatrix}, \begin{bmatrix} 1 \\ 0.5 \end{bmatrix} \right\}, \text{ so that } I = 4.$$

Note that we set the minimum input for the mRNA degradation to $0.5 > 0$ to avoid unboundedness. With these input choices it is intuitive that the largest possible state is reached when the mRNA production is at its maximum and the mRNA degradation is at its minimum. Therefore, in the MILPs we can use the bound $\mathbf{M} = x\,(T; 0, u(t) = \left[\begin{smallmatrix} 1 \\ 0.5 \end{smallmatrix}\right] \forall t)$. Fig. 5b) shows a comparison of the output reachable set for the case of two inputs versus the one input studied in part 1).

In Fig. 5b) we also compare the obtained reachable set with the reachable set computed using the function 'nonlinearSys' of the CORA toolbox (grey area). Note that the function 'nonlinearSys' is designed for generic nonlinear systems with inputs taking value in a continuous interval. The method in Section V-A2, on the other hand, is tailored to biological systems with discrete external signals, leading to (16). For running 'nonlinearSys' we optimised the parameters timeStep, taylorTerms, zonotopeOrder in the intervals $\{0.05, 0.1, 0.5\}$, $\{4, 6\}$, $\{200, 400, 600, 800, 1000, 1200\}$, the other parameters were set as in Section 12.1.3 of the CORA manual 2016. The running time of our algorithm is 77.7076 seconds, the one of CORA is 46.1436 seconds. One can see that even though CORA is faster, the reachable set obtained with the method of Section V-A2 is more precise. This discrepancy may be partially due to the fact that CORA assumes continuous input sets while we use discrete inputs. Nonetheless the set computed by CORA includes negative values, while mean and variance are always positive. Moreover, the black crosses in Figure 5b) are computed by simulating the system with *continuous input sets*, suggesting that the reachable sets with continuous and discrete inputs may be identical.

3) Fluorescent protein and experimental data: The way researchers typically measure the amount of proteins produced by a cell is by tagging it with a fluorescent marker. To model this scenario, we assume that 1) the protein P can mature into a fluorescent protein F according to the additional maturation and degradation reactions

$$P \xrightarrow{\alpha_5(k_f, z)} F, \qquad F \xrightarrow{\alpha_6(\gamma_p, z)} \emptyset,$$

where $\alpha_5(k_f, z) := k_f \cdot p, \quad \alpha_6(\gamma_p, z) := \gamma_p \cdot f$, $k_f > 0$ is the maturation rate and, for simplicity, the degradation rate of F is assumed to be the same as that of P; 2) the fluorescence intensity $I(t)$ of each cell can be measured and is proportional to the amount of fluorescence protein, that is, $I(t) = rF(t)$ for a fixed scaling parameter $r > 0$.

Since all the propensities are affine, the system describing the evolution of means and variances of such augmented network is

$$\dot{x}_{\leq 2}(t) = A^f(u(t))x_{\leq 2}(t) + b^f(u(t)), \tag{39}$$

where the state vector $x_{\leq 2}(t)$ and $A^f(u(t)), b^f(u(t))$ are

$$x_{\leq 2} = [\mathbb{E}[M], \mathbb{E}[P], \mathbb{E}[F], \mathbb{V}[M, P], \mathbb{V}[M, F], \mathbb{V}[P], \mathbb{V}[P, F], \mathbb{V}[F]]^\top$$

$$A^f = \begin{bmatrix} d_1(u_2(t)) & 0 & 0 & 0 & 0 & 0 & 0 & 0 \\ k_p & d_2 & 0 & 0 & 0 & 0 & 0 & 0 \\ 0 & \gamma_p & d_3 & 0 & 0 & 0 & 0 & 0 \\ k_p & 0 & 0 & d_4(u_2(t)) & 0 & 0 & 0 & 0 \\ 0 & 0 & 0 & \gamma_p & d_5(u_2(t)) & 0 & 0 & 0 \\ k_p & (\gamma_p + k_f) & 0 & 2k_p & 0 & d_6 & 0 & 0 \\ 0 & -\gamma_p & 0 & 0 & k_p & \gamma_p & d_7 & 0 \\ 0 & \gamma_p & k_f & 0 & 0 & 0 & 2\gamma_p & d_8 \end{bmatrix},$$

$$b^f = \begin{bmatrix} k_r u_1(t) & 0 & 0 & 0 & 0 & 0 & 0 & 0 \end{bmatrix}^\top$$

with $d_1(u_2(t)) = -\gamma_r u_2(t),\ d_2 = -(\gamma_p + k_f),\ d_3 = -k_f,$ $d_4(u_2(t)) = -(\gamma_r u_2(t) + \gamma_p + k_f), d_5(u_2(t)) = -(\gamma_r u_2(t) + k_f),$ $d_6 = -2(\gamma_p + k_f),\ d_7 = -(2k_f + \gamma_p),\ d_8 = -2k_f.$

System (39) depends on the parameter vector $\theta = [k_r, \gamma_r, k_p, \gamma_p, k_f, r]$ (for more details see [62, Supplementary Information pg. 16]). For the parameters we use the MAP estimates identified in [23] (all in min^{-1})

$$\begin{array}{lll} k_r = 0.0236 & \gamma_r = 0.0503 & k_p = 178.398 \\ k_f = 0.0212 & \gamma_p = 0.0121 & r^{-1} = 646.86 \end{array} \tag{40}$$

and we set $L^f = [re_3, r^2 e_8]^\top$ to compute the mean and variance reachable set for the fluorescence intensity.

Our first aim is to compare the reachable set of such extended model with experimental data, when only one external signal ("1in") is available. In the case of one input, (39) is a linear system and the methods of Section V-A1 can be applied. Fig. 6a) shows the estimated reachable set compared with the real data collected in [2] and with the reachable set computed using the 'linearSys' function of CORA for the settings timeStep=1, taylorTerms=4, zonotopeOrder=200. The simulation time was 4.1279 seconds with the method of Section V-A1 and 3.6891 seconds with CORA.

Our second goal is to investigate how the reachable set changes when both mRNA production and degradation are controlled ("2in"), as studied in [9]. In this case, system (39) is nonlinear. We therefore set $T = 300$ min and assume that switchings can occur every 20 min, so that Assumption 3 is satisfied with $K = 15$ and use the hyperplane method as described in Section V-A2 with input set Σ^{2in} as in Section VII-A2. Fig. 6b) shows a comparison of the reachable sets obtained for one and two external signals. Solving the MILP reformulation of problem (11), for such $n = 8$ dimentional system, took on average 20.6204 minutes per direction (minimum=0.1749 sec and maximum=135.2263 min). Overall, the simulation time for computing the outer approximation with the hyperplane method was 7.5 hrs. Computing the exact reachable set by simulating all the possible switching signals, assuming that one simulation takes 10^{-4} sec and neglecting the time needed to enumerate all possible signals, would take 29.8 hrs. Computing the reachable set with the function 'nonlinearSys' of CORA is significantly faster (of the order of tens of minutes depending on the settings), but leads to an overly conservative approximation (that includes the grey region shown in Fig. 6b) as well as negative values). The black crosses in Fig. 6b) are obtained by simulating the output of the system for 5000 randomly constructed input

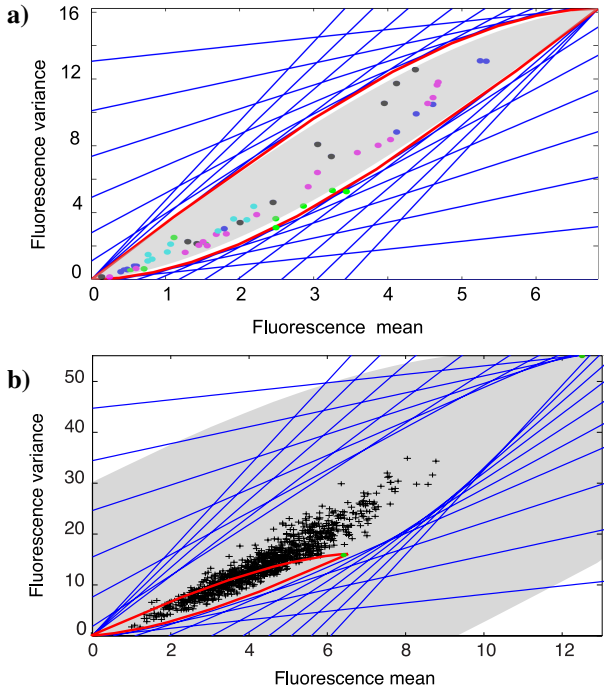

Fig. 6. Output reachable set of system (39) with output given by $y = L^f x$ and parameters as in (40). *Figure a) [1 external signal]:* Comparison between the measured data and the inner (red contour) and outer (blue lines) approximation of the output reachable set, for the case "1in". Different colors refers to data collected in different experiments. The grey area is the outer approximation computed using CORA. *Figure b) [2 external signals]:* Outer approximation of the output reachable set, for the case "2in". The two green dots represent the outputs when $u(t) = [1, 0.5]^\top \ \forall t$ and $u(t) = [1, 1]^\top \ \forall t$, respectively. The black crosses represent the output for random signals in $\Sigma^{2\text{in}}$. The red solid line is the outer approximation obtained for one external signal, as in Fig. a). The grey area shows the part of the outer approximation computed using CORA that lies in the positive orthant (CORA approximation includes negative regions not shown here because they are not physically relevant).

signals. This simulation illustrates that random approaches might lead to significantly underestimate the reachable set.

B. Non-closed moment equations

1) Single input and saturation: We consider again Example 2, but we now assume that not all the reactions follow the laws of mass action kinetics. Specifically, we are interested in investigating how the reachable set changes if we assume that the number of ribosomes in the cell is limited and consequently we impose a saturation to the translation propensity. Following [63], we assume that the translation rate follows the Michaelis-Menten kinetics so that

$$\alpha_3(k_p, z) = \tilde{k}_p \cdot \tfrac{a \cdot m}{b + a \cdot m} \quad \text{instead of} \quad \alpha_3(k_p, z) = k_p \cdot m.$$

For the simulations we impose $\tilde{k}_p = 0.7885, b = 0.06, a = 0.02$, so that the maximum reachable protein mean is the same as in the case without saturation analysed in the previous subsection. The corresponding propensity function is illustrated in Fig. 7a). All the other propensities are assumed as in Section VII-A1. Note that in this case the propensities are not affine. Consequently, we estimate the reachable set by using the FSP approach derived in Theorem 3. Specifically we consider as set J the indices corresponding to states with no more than 6 mRNA copies and 40 protein copies. This choice leads to a switched system as in (16) of dimension $n = 287$. By assuming $T = 360$ min and that u can switch any 30 minutes in the set $\Sigma^d = \{0, 1\}$, we obtain an error $\varepsilon = 2.84 \cdot 10^{-4}$ (this error can be computed by solving an MILP as explained in Remark 4). For each direction, the MILP reformulation of problem (11) was solved by Gurobi on average in 63.2317 minutes (minimum: 49 sec and maximum: 216.7833 min). Fig. 7b) shows the comparison of the reachable sets obtained for the cases with and without saturation. From this plot it emerges that, for the chosen values of parameters, saturation leads to a decrease of variability in the population.

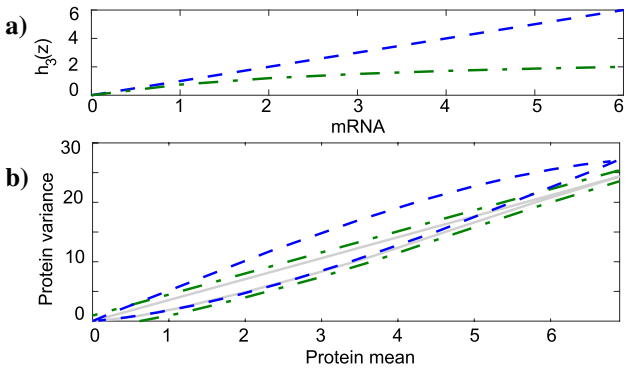

Fig. 7. Comparison of the reachable set for the protein mean and variance, according to the model in Example 2, when all the reactions follows the mass action kinetics (as in Fig 5a)) and when the translation is saturated. *Figure a):* $h_3(z)$ when the translation reaction follows the mass action kinetics (dashed blue) or the Michaelis Menten kinetics (dashed dotted green). *Figure b):* comparison of the outer approximations of the reachable sets in the two cases. The blue dashed line is as in Fig 5a). The grey line is the outer approximation of the reachable set of the FSP system (28), the green dashed dotted line is the outer approximation of the original system (27) according to Theorem 3.

2) Bimolecular reactions and controlled promoter switching: As the last case study we consider a system with bimolecular reactions, as studied in [10], with an additional layer of complexity given by the presence of a controlled promoter. Specifically, we assume that a certain gene switches stochastically between a OFF and ON state, according to the following reactions

$$OFF \xrightarrow{\sigma} ON, \qquad ON \xrightarrow{\gamma_{OFF}} OFF,$$

where $\sigma \in \{0, 1\}$ is the external signal and γ_{OFF} is the rate at which the gene turns naturally off. Controlled promoter switching of this type can be obtained for example using the lactose operon [64]. We then assume that when the gene is on it produces a protein S_1, which can dimerise into S_2 according to the reaction network

$$\begin{aligned} ON &\xrightarrow{k_1} ON + S_1, & S_1 + S_1 &\xrightarrow{b} S_2, \\ S1 &\xrightarrow{\gamma_1} \emptyset, & S_2 &\xrightarrow{\gamma_2} \emptyset. \end{aligned}$$

This latter network is as in [10]. For our simulations we used the parameters found therein, that is, $b = 3, \gamma_1 = 2, \gamma_2 = 1$. We also set $k_1 = 20, \gamma_{OFF} = 0.2$. We used a set J such that $S_1 \in \{0, \dots, 10\}$, $S_2 \in \{0, \dots, 20\}$, $ON, OFF \in \{0, 1\}$. Note that since the promoter is always either ON or OFF, we also imposed that $ON + OFF = 1$. The resulting switched system has dimension $n = 462$. The corresponding reachable set, for S_2 and $T = 12$ with possible input switching every time unit, is illustrated in Fig. 8. Solving the MILP for each direction took on average 113.8 minutes (minimum: 1.5481

min and maximum: 254.8 min). The associated error was computed as in Remark 4 and was $\varepsilon = 0.0012$.

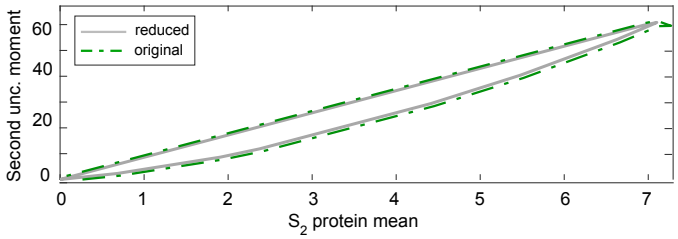

Fig. 8. Reachable set for the mean and second moment of S_2 in the system of Section VII-B2, starting from a promoter in the OFF state. The grey line is the outer approximation of the reachable set of the FSP system (28), the green dashed dotted line is the outer approximation of the original system (27) according to Theorem 3.

VIII. Conclusion

In the paper we have: i) proposed a method to approximate the projected reachable set of switched affine systems with fixed switching times, ii) extended the FSP approach to controllable networks, iii) illustrated how these new theoretical tools can be used to analyse generic networks both from a population and single cell perspective and iv) provided an extensive gene expression case study using both in silico and in vivo data. Even though our analysis is motivated by biochemical reaction networks, our results can actually be applied to study the moments of any Markov chain with transitions rates that switch among I possible configurations at K fixed instants of times. Our results hold both in case of finite and infinite state space. Finally, we note that the reachability method derived here could be useful for the analysis of switched systems with the structure described in Section III-B, even outside the systems biology domain. To this end, a more thorough computational study is needed.

References

[1] A. Milias-Argeitis, S. Summers, J. Stewart-Ornstein, I. Zuleta, D. Pincus, H. El-Samad, M. Khammash, and J. Lygeros, "In silico feedback for in vivo regulation of a gene expression circuit," *Nature Biotechnology*, vol. 29, pp. 1114–1116, 2011.

[2] J. Ruess, F. Parise, A. Milias-Argeitis, M. Khammash, and J. Lygeros, "Iterative experiment design guides the characterization of a light-inducible gene expression circuit," *National Academy of Sciences of the USA*, vol. 112, no. 26, pp. 8148–8153, 2015.

[3] E. J. Olson, L. A. Hartsough, B. P. Landry, R. Shroff, and J. J. Tabor, "Characterizing bacterial gene circuit dynamics with optically programmed gene expression signals." *Nature Methods*, vol. 11, pp. 449–455, 2014.

[4] J. Uhlendorf, A. Miermont, T. Delaveau, G. Charvin, F. Fages, S. Bottani, G. Batt, and P. Hersen, "Long-term model predictive control of gene expression at the population and single-cell levels." *National Academy of Sciences of the USA*, vol. 109, no. 35, pp. 14 271–14 276, 2012.

[5] F. Menolascina, M. Di Bernardo, and D. Di Bernardo, "Analysis, design and implementation of a novel scheme for in-vivo control of synthetic gene regulatory networks," *Automatica*, pp. 1265–1270, 2011.

[6] G. Batt, H. De Jong, M. Page, and J. Geiselmann, "Symbolic reachability analysis of genetic regulatory networks using discrete abstractions," *Automatica*, vol. 44, no. 4, pp. 982–989, 2008.

[7] N. Chabrier and F. Fages, "Symbolic model checking of biochemical networks," in *Computational Methods in Systems Biology*, C. Priami, Ed. Springer, 2003, pp. 149–162.

[8] D. T. Gillespie, "A rigorous derivation of the chemical master equation," *Physica A: Statistical Mechanics and its Applications*, pp. 404–425, 1992.

[9] C. Briat and M. Khammash, "Computer control of gene expression: Robust setpoint tracking of protein mean and variance using integral feedback," in *IEEE CDC*, 2012, pp. 3582–3588.

[10] ——, "Integral population control of a quadratic dimerization process," in *Decision and Control (CDC), 2013 IEEE 52nd Annual Conference on*. IEEE, 2013, pp. 3367–3372.

[11] C. Briat, C. Zechner, and M. Khammash, "Design of a synthetic integral feedback circuit: Dynamic analysis and DNA implementation," *ACS Synthetic Biology*, 2016.

[12] I. Lestas, G. Vinnicombe, and J. Paulsson, "Fundamental limits on the suppression of molecular fluctuations," *Nature*, pp. 174–178, 2010.

[13] W. J. Blake, G. Balázsi, M. A. Kohanski, F. J. Isaacs, K. F. Murphy, Y. Kuang, C. R. Cantor, D. R. Walt, and J. J. Collins, "Phenotypic consequences of promoter-mediated transcriptional noise," *Molecular cell*, vol. 24, no. 6, pp. 853–865, 2006.

[14] A. M. Arias and P. Hayward, "Filtering transcriptional noise during development: concepts and mechanisms," *Nature reviews. Genetics*, vol. 7, no. 1, p. 34, 2006.

[15] A. Sanchez, S. Choubey, and J. Kondev, "Regulation of noise in gene expression," *Annual review of biophysics*, vol. 42, pp. 469–491, 2013.

[16] T. J. Graettinger and B. H. Krogh, "Hyperplane method for reachable state estimation for linear time-invariant systems," *Journal of optimization theory and applications*, vol. 69, no. 3, pp. 555–588, 1991.

[17] J. T. Linderoth and A. Lodi, "Milp software," *Wiley encyclopedia of operations research and management science*, 2010.

[18] P. Bonami, M. Kilinç, and J. Linderoth, "Algorithms and software for convex mixed integer nonlinear programs," *Mixed integer nonlinear programming*, pp. 1–39, 2012.

[19] B. Munsky and M. Khammash, "The finite state projection algorithm for the solution of the chemical master equation." *The Journal of chemical physics*, vol. 124, no. 4, p. 044104, 2006.

[20] C. Baier, B. Haverkort, H. Hermanns, and J.-P. Katoen, "Model-checking algorithms for continuous-time Markov chains," *IEEE Trans. on Software Engineering*, vol. 29, no. 6, pp. 524–541, 2003.

[21] A. Abate, J.-P. Katoen, J. Lygeros, and M. Prandini, "Approximate model checking of stochastic hybrid systems," *European Journal of Control*, vol. 16, no. 6, pp. 624–641, 2010.

[22] H. El-Samad, S. Prajna, A. Papachristodoulou, J. Doyle, and M. Khammash, "Advanced methods and algorithms for biological networks analysis," *IEEE*, vol. 94, no. 4, pp. 832–853, 2006.

[23] F. Parise, M. E. Valcher, and J. Lygeros, " On the use of hyperplane methods to compute the reachable set of controlled stochastic biochemical reaction networks," in *IEEE CDC*, 2015, pp. 1259–1264.

[24] ——, "Reachability analysis for switched affine autonomous systems and its application to controlled stochastic biochemical reaction networks," in *IEEE CDC*, 2016.

[25] D. Liberzon, *Calculus of variations and optimal control theory: A concise introduction*. Princeton University Press, 2011.

[26] H. J. Sussmann, "Lie Brackets, Real Analyticity and Geometric Control," in *Differential Geometric Control Theory*, R. W. Brockett, R. S. Millman, and H. J. Sussmann, Eds. Birkhauser Boston, 1983, vol. 27, pp. 1–116.

[27] C. Seatzu, D. Corona, A. Giua, and A. Bemporad, "Optimal control of continuous-time switched affine systems," *IEEE Trans. on Automatic Control*, vol. 51, no. 5, pp. 726–741, 2006.

[28] A. Bemporad and M. Morari, "Control of systems integrating logic, dynamics, and constraints," *Automatica*, pp. 407–427, 1999.

[29] A. Girard and C. Le Guernic, "Efficient reachability analysis for linear systems using support functions," *IFAC Proceedings Volumes*, vol. 41, no. 2, pp. 8966–8971, 2008.

[30] P. Varaiya, "Reach set computation using optimal control," in *Verification of Digital and Hybrid Systems*. Springer, 2000, pp. 323–331.

[31] C. Le Guernic and A. Girard, "Reachability analysis of linear systems using support functions," *Nonlinear Analysis: Hybrid Systems*, vol. 4, no. 2, pp. 250–262, 2010.

[32] M. Althoff and G. Frehse, "Combining zonotopes and support functions for efficient reachability analysis of linear systems," in *IEEE CDC*, 2016, pp. 7439–7446.

[33] A. Lotov, V. A. Bushenkov, and G. K. Kamenev, *Interactive decision maps: Approximation and visualization of Pareto frontier*. Springer Science & Business Media, 2013, vol. 89.

[34] E. Asarin and T. Dang, "Abstraction by projection and application to multi-affine systems," in *International Workshop on Hybrid Systems: Computation and Control*. Springer, 2004, pp. 32–47.

[35] C. Le Guernic and A. Girard, "Reachability analysis of hybrid systems using support functions." in *CAV*. Springer, 2009, pp. 540–554.

[36] W. Hagemann, "Reachability analysis of hybrid systems using symbolic orthogonal projections," in *International Conference on Computer Aided Verification*. Springer, 2014, pp. 407–423.

[37] G. Frehse, C. Le Guernic, A. Donzé, S. Cotton, R. Ray, O. Lebeltel, R. Ripado, A. Girard, T. Dang, and O. Maler, "Spaceex: Scalable verification of hybrid systems," in *Computer Aided Verification*. Springer, 2011, pp. 379–395.

[38] M. R. Greenstreet, "Verifying safety properties of differential equations," in *International Conference on Computer Aided Verification*. Springer, 1996, pp. 277–287.

[39] T. Dang and O. Maler, "Reachability analysis via face lifting," *Hybrid Systems: Computation and Control*, pp. 96–109, 1998.

[40] O. Stursberg and B. H. Krogh, "Efficient representation and computation of reachable sets for hybrid systems," in *International Workshop on Hybrid Systems: Computation and Control*. Springer, 2003, pp. 482–497.

[41] A. Kurzhanski and I. Valyi, *Ellipsoidal calculus for estimation and control*. Springer, 1997.

[42] O. Botchkarev and S. Tripakis, "Verification of hybrid systems with linear differential inclusions using ellipsoidal approximations," in *HSCC*. Springer, 2000, pp. 73–88.

[43] A. A. Kurzhanskiy and P. Varaiya, "Ellipsoidal techniques for reachability analysis of discrete-time linear systems," *IEEE Transactions on Automatic Control*, vol. 52, no. 1, pp. 26–38, 2007.

[44] A. B. Kurzhanski and P. Varaiya, "Ellipsoidal techniques for hybrid dynamics: the reachability problem," *New Directions and Applications in Control Theory*, pp. 193–205, 2005.

[45] A. Chutinan and B. H. Krogh, "Verification of polyhedral-invariant hybrid automata using polygonal flow pipe approximations," in *International workshop on hybrid systems: computation and control*. Springer, 1999, pp. 76–90.

[46] E. Asarin, O. Bournez, T. Dang, and O. Maler, "Approximate reachability analysis of piecewise-linear dynamical systems," in *International Workshop on Hybrid Systems: Computation and Control*. Springer, 2000, pp. 20–31.

[47] A. Girard, "Reachability of uncertain linear systems using zonotopes," in *HSCC*, vol. 5. Springer, 2005, pp. 291–305.

[48] A. Girard, C. Le Guernic, and O. Maler, "Efficient computation of reachable sets of linear time-invariant systems with inputs," in *International Workshop on Hybrid Systems: Computation and Control*. Springer, 2006, pp. 257–271.

[49] E. Lakatos and M. Stumpf, "Control mechanisms for stochastic biochemical systems via computation of reachable sets," *bioRxiv*, 2016.

[50] F. Parise, M. E. Valcher, and J. Lygeros, "On the reachable set of the controlled gene expression system," in *IEEE CDC*, 2014, pp. 4597–4604.

[51] C. Yan and M. Greenstreet, "Faster projection based methods for circuit level verification," in *Proceedings of the 2008 Asia and South Pacific Design Automation Conference*. IEEE Computer Society Press, 2008, pp. 410–415.

[52] D. J. Wilkinson, *Stochastic modeling for systems biology*. CRC, 2011.

[53] J. Goutsias and G. Jenkinson, "Markovian dynamics on complex reaction networks," *Physics Reports*, vol. 529, no. 2, pp. 199–264, 2013.

[54] J. Ruess, "Moment-based methods for the analysis and identification of stochastic models of biochemical reaction networks." *Doctoral dissertation, ETH Zurich*, 2014.

[55] J. Hespanha, "Moment closure for biochemical networks," in *IEEE International Symposium on Communications, Control and Signal Processing*, 2008, pp. 142–147.

[56] C. H. Lee, K.-H. Kim, and P. Kim, "A moment closure method for stochastic reaction networks," *The Journal of Chemical Physics*, vol. 130, no. 13, p. 134107, 2009.

[57] S. Engblom, "On the stability of stochastic jump kinetics," *arXiv preprint arXiv:1202.3892*, 2012.

[58] M. Rathinam, "Moment growth bounds on continuous time markov processes on non-negative integer lattices," *arXiv:1304.5169*, 2013.

[59] A. Gupta, C. Briat, and M. Khammash, "A scalable computational framework for establishing long-term behavior of stochastic reaction networks," *PLoS computational biology*, vol. 10, no. 6, 2014.

[60] I. Gurobi Optimization, "Gurobi optimizer reference manual," 2016. [Online]. Available: http://www.gurobi.com

[61] M. Althoff, "An introduction to CORA 2015," in *Proc. of the Workshop on Applied Verification for Continuous and Hybrid Systems*, 2015, pp. 120–151.

[62] J. Ruess, A. Milias-Argeitis, and J. Lygeros, "Designing experiments to understand the variability in biochemical reaction networks." *Journal of the Royal Society Interface*, vol. 10, no. 88, p. 20130588, 2013.

[63] R. Brockmann, A. Beyer, J. J. Heinisch, and T. Wilhelm, "Posttranscriptional expression regulation: what determines translation rates?" *PLoS Comput Biol*, vol. 3, no. 3, p. e57, 2007.

[64] T. Kuhlman, Z. Zhang, M. H. Saier, and T. Hwa, "Combinatorial transcriptional control of the lactose operon of escherichia coli," *PNAS*, vol. 104, no. 14, pp. 6043–6048, 2007.

Francesca Parise Francesca Parise was born in Verona, Italy, in 1988. She received the B.Sc. and M.Sc. degrees (cum Laude) in Information and Automation Engineering from the University of Padova, Italy, in 2010 and 2012, respectively. She conducted her master thesis research at Imperial College London, UK, in 2012. She graduated from the Galilean School of Excellence, University of Padova, Italy, in 2013. She defended her PhD at the Automatic Control Laboratory, ETH Zurich, Switzerland in 2016 and she is currently a Postdoctoral researcher at the Laboratory for Information and Decision Systems, M.I.T., USA. Her research interests include game theory, distributed control and analysis of complex systems, with application to distributed multi-agent networks and systems biology.

Maria Elena Valcher Maria Elena Valcher received the Laurea degree and the PhD from the University of Padova, Italy. Since January 2005 she is full professor of Automatica at the University of Padova.

She is author/co-author of 76 papers appeared in international journals, 92 conference papers, 2 text-books and several book chapters. Her research interests include multidimensional systems theory, polynomial matrix theory, behavior theory, convolutional coding, fault detection, delay-differential systems, positive systems, positive switched systems and Boolean control networks. She has been involved in the Organizing Committees and in the Program Committees of several conferences. In particular, she was the Program Chair of the CDC 2012. She was in the Editorial Board of the IEEE Transactions on Automatic Control (1999-2002), Systems and Control Letters (2004-2010) and she is currently in the Editorial Boards of Automatica (2006-today), Multidimensional Systems and Signal Processing (2004-today), SIAM J. on Control and Optimization (2012-today), European Journal of Control (2103-today) and IEEE Access (2014-today). She was Appointed Member of the CSS BoG (2003); Elected Member of the CSS BoG (2004-2006; 2010-2012); Vice President Member Activities of the CSS (2006-2007); Vice President Conference Activities of the CSS (2008-2010); CSS President (2015). She is presently a Distinguished Lecturer of the IEEE CSS and IEEE CSS Past President. She received the 2011 IEEE CSS Distinguished Member Award and she is an IEEE Fellow since 2012.

John Lygeros John Lygeros completed a B.Eng. degree in electrical engineering in 1990 and an M.Sc. degree in Systems Control in 1991, both at Imperial College of Science Technology and Medicine, London, U.K.. In 1996 he obtained a Ph.D. degree from the Electrical Engineering and Computer Sciences Department, University of California, Berkeley. During the period 1996-2000 he held a series of research appointments at the National Automated Highway Systems Consortium, Berkeley, the Laboratory for Computer Science, M.I.T., and the Electrical Engineering and Computer Sciences Department at U.C. Berkeley. Between 2000 and 2003 he was a University Lecturer at the Department of Engineering, University of Cambridge, U.K., and a Fellow of Churchill College. Between 2003 and 2006 he was an Assistant Professor at the Department of Electrical and Computer Engineering, University of Patras, Greece. In July 2006 he joined the Automatic Control Laboratory at ETH Zurich, first as an Associate Professor, and since January 2010 as a Full Professor. Since 2009 he is serving as the Head of the Automatic Control Laboratory and since 2015 as the Head of the Department of Information Technology and Electrical Engineering. His research interests include modelling, analysis, and control of hierarchical, hybrid, and stochastic systems, with applications to biochemical networks, automated highway systems, air traffic management, power grids and camera networks. He teaches classes in the area of systems and control both at the undergraduate and at the graduate level at ETH Zurich, notably the 4th semester class Signals and Systems II, which he delivers in a flipped classroom format. John Lygeros is a Fellow of the IEEE, and a member of the IET and the Technical Chamber of Greece. He served as an Associate Editor of the IEEE Transactions on Automatic Control and in the IEEE Control Systems Society Board of Governors; he is currently serving as the Treasurer of the International Federation of Automatic Control.